Authors' response to Martin Gysel

We would like to thank Martin Gysel for his thorough comments and valuable suggestions regarding our manuscript. Based on these comments we have made modifications to our manuscript and slightly changed the analysis method and data presentation. These changes are addressed below with reviewer's comments written in italics and followed by authors' responses (normal font).

This study investigates the role of aerosol hygroscopicity on its ability to form cloud droplets. Many previous studies have addressed the roles played by particle size and particle hygroscopicity on the ability of such particles to act as cloud condensation nuclei (CCN). However, this was for the most part done based on theoretical considerations, laboratory studies and/or simulated droplet formation on ambient aerosol in CCN counters. This study is one of very few studies that directly investigated the activation of aerosol into the droplets of atmospheric clouds as a function of their size and hygroscopicity. State-of-the-art experimental methods were applied to independently determine the hygroscopicity distributions of the total aerosol and the interstitial aerosol, based on which they could clearly show that the less hygroscopic particles are much less efficient in forming cloud droplets compared to the more hygroscopic particles of equal size. While this essentially confirms expectations, it is still a very valuable result as it directly affects how local/regional emissions contribute to cloud droplet number and to what extent the less hygroscopic particles can be processed by clouds.

The manuscript is generally well written, concise and within the scope of ACP. The data analysis approaches seem appropriate for the most part. However, in two cases I am not sure whether the results are internally consistent. Besides, one figure, which is essentially just an internal consistency check of the data analysis approaches, comes as if it was an independent result (see major comments). The "minor comments" are largely just meant to clarify e few things, to improve the notation in equations in order to avoid ambiguities and to provide several ideas for additional analyses. I do not expect that the latter should all be addressed in a comprehensive manner (nor would I expect exhaustive rebuttals for most of them).

In conclusion, I recommend this interesting and relevant manuscript for publication in ACP after the most relevant comments have been addressed by the authors.

Major comments:

1. **Comment:** *P.8, l.21-22:"Typically, the activation efficiencies calculated by Eq. (9) ($f_{act,GF>0.80}$) appeared somewhat larger than the DMPS derived values ($f_{act,DMPS}$)." – I claim that this is impossible! It must be caused by errors in the calculations (e.g. from inconsistent choice of GF-PDF normalization approach and integration of the GF-PDFs in Equation 9 or from comparing at different times). Let me explain: "GF>0.80" means that you integrate over the whole GF-range of the GF-PDF. The fact that the GF-PDF, as used in Equation 9, must be normalized to unit area, directly implies that, for "GF>0.80", Equation 9 simplifies to*

   $$f_{act,GF>0.80}(Dp) = (dN_{tot}(Dp)/dlogDp - dN_{int}(Dp)/dlogDp) / dN_{tot}(Dp)/dlogDp$$

   and this is nothing else than how I would define $f_{act,DMPS}(D_p)$. Or in other words: there is no more HTDMA derived information left in $f_{act,GF>0.80}(D_p)$, only DMPS-derived information. Therefore the poor time resolution or other potential issues with the HTDMA measurement cannot influence the

result. Please reconsider your calculations and add the results from all other available measurements to Table 1 too, if there was really a mistake in the previous approach.

Response: In the original manuscript, the GF-PDF "scaling factors" were derived from HTDMA measurements, and therefore, all the $f_{act,GF}$ values were independent from DMPS measurements. We agree that this was quite poorly expressed in the text. However, we have re-considered our calculations and decided to change the analysis so that the scaling factors are now derived from DMPS measurements.

As the reviewer pointed out, this should result in equal $f_{act,DMPS}$ and $f_{act,GF>0.80}$ (in the case that $f_{act,GF>0.80}$ is determined by integrating over the whole GF range). However, due to issues with time resolution and relatively slow alteration between the two sampling lines, $f_{act,GF<1.25}$ can sometimes appear negative. Please see our response to comment #2 for further details on this issue.

After revising the calculations, we have decided to include one more cloud event in the manuscript. We also found a small mistake in the analysis as the starting time of event #1 (now event #2) was miscopied as 20:35 instead of 20:25. We have updated Table 1 and revised the related discussion accordingly.

2. **Comment:** *Table 1: Shouldn't the following equality hold for the data shown in Table 1?*

$$f_{act,GF>0.80}(D_p) = f_{GF<1.25}(D_p) * f_{act,GF<1.25}(D_p) + (1 - f_{GF<1.25}(D_p))* f_{act,GF>1.25}(D_p)$$

(simply use Equation 9 to get this). It does seem to be fulfilled for some columns of Table 1 but not for others. Please check your data or clarify the manuscript if I misinterpreted the meaning of Equation 9 or f_{act} or so.

Response: This is a good point and this issue should have been addressed in the manuscript. Ideally, if the activated fraction is zero, the interstitial and total particle concentrations should be equal. However, as the measurements are not done simultaneously, the interstitial concentrations can be occasionally higher than the respective total concentrations. Thus, the activation efficiencies calculated by Eq. (9) (now, Eq. 10) can become negative.

In the original manuscript, these values were reported as zeros but treated as negative when calculating the total activated fractions ($f_{act,GF>0.80}$). By contrast, in the revised version, the negative activation efficiencies are treated as zeros in order to reach consistent values for $f_{act,GF<1.25}$, $f_{act,GF>1.25,}$ and $f_{act,GF>0.80.}$ On the other hand, this may (again) cause small differences between $f_{act,GF>0.80}$ and $f_{act,DMPS}$.

The following sentences are now added to the manuscript right after the Eq. (10):

> "Here it should be noted that the activation efficiencies can appear negative if the averaged interstitial concentrations are higher than the corresponding total values. This can be the case especially within the less hygroscopic regime where the activated fractions are generally low. In such cases, the negative activation efficiencies are reported as zeros and treated as such when calculating the total activated fractions ($f_{act,GF\geq0.80}$). Thus, the resulting $f_{act,GF\geq0.80}$ values can be slightly different from the ones derived solely from DMPS measurements. ".

3. **Comment:** *Figure 3 and first paragraph of Section 3.4:*

The comparison of cloud droplet predictions made with considering the hygroscopic mixing state or with assuming internal mixture (and using κ_{avg}) is useful, as it confirms previous results on the sensitivity of CCN predictions to simplified treatment of mixing state for the effect of mixing state of total cloud droplet concentration in real clouds.

By contrast, the comparison of HTDMA+$DMPS_{tot}$+$S_{c,eff}$-predictions of cloud droplet number concentration with those derived from the $DMPS_{tot}$ minus $DMPS_{int}$ measurements is meaningless because it is circular argumentation! Equation 8 was first used to infer the $S_{c,eff}$ from the HTDMA, $DMPS_{tot}$ and $DMPS_{int}$ *measurements. The $S_{c,eff}$ obtained in this manner was then used, along with the HTDMA + $DMPS_{tot}$ data, for cloud droplet prediction to be compared with those derived from $DMPS_{tot}$ minus $DMPS_{int}$ measurements as shown in Figure 3. Consequently, this analysis has nothing to do with a closure study, instead it is simply an internal consistency check of the approach to infer $S_{c,eff}$ and to predict cloud droplet number. Therefore, this part of the figure (i.e. the red data points) has to be removed and the discussion needs to be adapted.*

Response: Again, this is very good point and we agree that we are not presenting any closure results in Fig. 3. In our opinion, however, this self-consistency check should be included in the paper as it serves a justification/base for the results presented in Sect. 3.5.

In Sect. 3.5, the cloud droplet concentrations are estimated with an assumption that only the more hygroscopic particles were present in the atmosphere. Thereafter, these values are compared to those shown in Fig. 3 (red points). Thus, the main purpose of Fig. 3 is just to assure that the simulated reference values/conditions are comparable to real ambient observations.

Keeping this in mind, we have added the following disclaimer to the manuscript:

> "Nevertheless, since the determination of $N_{act,HTDMA}$ included the estimation of effective peak supersaturation by means of $f_{act,DMPS}$, the comparison shown here can't be considered as a real CCN closure study in an explicit manner. Instead, it rather serves as a base for the analysis presented in the following section (Sect. 3.5)".

Comment: *Nevertheless, it is worth to have a closer look into Figure 3. The fact that the grey points have higher correlation and slope closer to unity than the red points is unexpected. If the cloud droplet prediction is so insensitive to assuming internal mixing state, why is then the "internal consistency check" of inferring and re-applying the effective supersaturation from/to the HTDMA measurements so poor (referring to slope and particularly the scatter of the red points)? Is this related to improper treatment of activation plateau values that differ from unity (see separate comment below concerning this potential issue)? Or is the minimization approach applied to infer the effective supersaturation (Equation 8) not suitable? Other reasons?*

Response: We apologize for the typo that we had on page 10, line 14. As it was marked in Fig. 3, the line fitted through the red data points had a slope of 1.016 instead on 1.03 (as it was mentioned in the text). It is true, however, that the grey dots had slightly higher R^2 than the red points. On the other hand, considering the reasonably low number of data points (n = 26) the difference (0.991 vs. 0.997) is practically negligible and should not be overinterpret.

It is also true that the measured activation curves did not always reach unity at larger sizes, whereas the HTDMA derived curves typically did. Therefore, it is definitely one possible explanation for the positive biases between $N_{act,HTDMA}$ and $N_{act,DMPS}$ ($N_{act,HTDMA} > N_{act,DMPS}$). We also tried an alternative minimization approach by simply minimizing the difference between the HTDMA and DMPS derived D50s, but the effect was negligible.

Minor comments:

4. **Comment:** *Abstract: Well written but for one missing element: The range of supersaturations occurring in the is not mentioned. This would be worthwhile as they appear to be rather low, which increases the sensitivity of CCN number concentration to hygroscopicity/composition compared to high supersaturation.*

   Response: The range of effective peak supersaturation is now included in the abstract.

5. **Comment:** *P.3, l.26: It might be worthwhile to mention how the visibility was measured.*

   Response: The weather sensors are now described in the manuscript.

6. **Comment:** *Sect. 2.3: A $PM_{1.0}$ impactor was used in the interstitial inlet to remove the activated cloud droplets just leaving the interstitial aerosol behind. However, the mode of none-activated droplets in stable equilibrium within the cloud may potentially extend to diameters larger than 1 µm, if the peak supersaturation at cloud formation was very low (the lower the peak supersaturation, the larger the activation cut-off diameter, the larger the maximal diameter of non-activated interstitial particles). In such a case, the largest and most hygroscopic particles of the true interstitial aerosol in the cloud would be missing in the aerosol sample measured behind the interstitial inlet. Hammer et al. (2014) address this issue in more detail. Can you exclude this potential artefact based on supporting data such as droplet size distributions or estimates of the maximal possible equilibrium droplet size for the clouds formed with the lowest peak supersaturation?*

   *Hammer, E., Gysel, M., Roberts, G. C., Elias, T., Hofer, J., Hoyle, C. R., Bukowiecki, N., Dupont, J.C., Burnet, F., Baltensperger, U., and Weingartner, E.: Size-dependent particle activation properties in fog during the ParisFog 2012/13 field campaign. Atmos. Chem. Phys., **14**, 1051710533, doi:10.5194/acp-14-10517-2014, 2014.*

   Response: This is a very good point and definitely something that we need to take into account in the future measurements. At this stage, however, we can neither exclude, nor quantify, the possible uncertainties inflicted to our observations.

7. **Comment:** *Sect. 2.4: The residence time between humidifier and DMA is provided (2s). The residence time within the humidifier might also be of interest, possibly even including a brief remark on the reasons for choosing a rather short or rather long residence time.*

Response: The residence time inside the humidifier was approximately 0.2 s. This piece of information is now added to the manuscript.

8. **Comment:** *Equation 2 and other instances in Sect. 2.5 and possibly the rest of the manuscript: This equation (Köhler-equation) describes the equilibrium water vapour saturation ratio (S_{eq}) as a function of particle hygroscopicity, diameter, etc. By contrast, the critical saturation ratio (S_c) is the maximum of the Köhler curve described with Equation 2. You are using the same symbol for these two different quantities. This needs to be fixed.*

   Response: Thank you for pointing out this mistake. S_c in Eq. (2) is now changed to S_{eq} and determined as an equilibrium saturation ratio. Later, S_c is defined as a critical saturation ratio and explained accordingly.

9. **Comment:** *Line just below Equation 3, "…where V_s and V_w are the soluble and water volumes…": In general, V_s is the volume of the whole dry particle, not just the soluble components. Insoluble fractions, if present, are accounted for with the κ-value.*

   Response: Good point. We have replaced V_s with V_p and rephrased the following definition as "…where V_p *and* V_w are the dry particle and water volumes…"

10. **Comment:** *Equation 5: This analytical solution for the critical saturation ratio contains mathematical approximations which become increasingly inaccurate with decreasing critical saturation ratio. Therefore, this equation should only be used for qualitative purposes, whereas a numerical solution of the Köhler equation must be implemented for quantitative purposes.*

    Response: This is also a good point, and therefore, Eq. (5) is now referred as an approximation. In addition, we repeated the simulations by solving the Köhler equation numerically. However, the effect was negligible and most likely compensated by very minor changes in the estimated $S_{c,eff}$ values.

11. **Comment:** *Equation 5 and line just below: This is now the critical saturation ratio. It should be explained what it is – in contrast to the equilibrium saturation ratio appearing in Equation 2 – and the symbol should be defined.*

    Response: Please see our response to comment 8.

12. **Comment***: Equations 6 and 7: It could be mentioned that the approach and equations used to predict the CCN number concentration from particle number size distribution (from SMPS) and GF-PDFs (from HTDMA) is identical to the approach introduced by Kammermann et al., 2010b (cf. their Equations 2&3).*

    Response: Reference to Kammermann et al. (2010b) is included.

13. **Comment:** *P.6, l. 5-8: This step also involves interpolation in time (besides inter-/extrapolation in size).*

    Response: Yes. Or alternatively, temporal averaging.

14. **Comment:** *P.6, l. 11ff: "Nonetheless, it has to be noted that above 200 nm, hygroscopicity is quite rarely a limiting factor and the most crucial activation characteristics are dependent on particle properties between the ~80 nm and ~200 nm sizes." – Isn't this statement somewhat in conflict with your result that a substantial portion of the non-hygroscopic particles remains interstitial (at the largest diameter covered by your measurements)? Therefore you need the additional argument that the number fraction of non-hygroscopic particles depends only weakly on size across the size range relevant in this context.*

    Response: This part of the text was indeed unclearly written. What we really wanted to state here was that according to the observed size dependence of $f_{GF<1.25}$, the particles at $D_p > 200$ nm were supposedly characterized by reasonably low number fractions of less hygroscopic particles. As a result, small uncertainties in the estimated GF-PDFs would only cause a small net bias to droplet predictions.

    Nevertheless, as we don't have actual measurement data for this size range (and this argument would be limited to average conditions at Puijo), we have decided to omit this statement from the manuscript.

15. **Comment:** *P.6, l.13ff: "Secondly, the method assumes that the subsaturated hygroscopicities are representative for supersaturated conditions. Such an assumption is not always totally valid and discrepancies between the two saturation regimes have been reported based on laboratory and field experiments…" – The study by Jurányi et al. (2013) could also be referenced here, as one of the examples that found very good closure between sub- and supersaturated regimes for externally mixed urban aerosol.*

    Response: We have added a reference to Jurányi et al. (2013).

16. **Comment:** *P6., l.19ff: Comments on the approach to estimate the effective peak supersaturation (PS: I'd suggest $S_{c,eff}$ rather than S_{eff} as symbol):*

    Response: S_{eff} and s_{eff} are replaced with $S_{c,eff}$ and $s_{c,eff}$ as suggested.

    a. *I suggest to start with a brief explanation of the concept behind estimating $S_{c,eff}$, possibly also referring to Hammer et al. (2014). This would be likely be helpful for the "average" reader of this manuscript.*

    Response: We have included a brief definition of $S_{c,eff}$ as well as a reference to Hammer et al. (2014).

b. *If entrainment occurs or in the case of partially/fully glaciated clouds the plateau value of $f_{act,DMPS}$, i.e. the value $f_{act,DMPS}$ takes at large diameters at which also the nonhygroscopic particle activate, may be substantially smaller than unity (e.g. Fig. 3 in Verheggen et al., 2007). The minimization approach given in Equation 8 would cause a bias for such a scenario. – Did you observe evidence for entrainment and/or glaciation or did the plateau value of $f_{act,DMPS}$ always reach unity?*

Verheggen, B., Cozic, J., Weingartner, E., Bower, K., Mertes, S., Connolly, P., Gallagher, M., Flynn, M., Choularton, T., and Baltensperger, U.: Aerosol partitioning between the interstitial and the condensed phase in mixed-phase clouds. J. Geophys. Res., ***112****, D23202, doi:10.1029/2007JD008714, 2007.*

Response: As we mentioned in our response to comment #3, the DMPS derived activation curves did not always reach unity. Thus, we can't fully exclude the possibility of entrainment. On the other hand, the reduced activation efficiency of larger particles was also associated with reasonably low particle concentrations (→ small deviations in particle concentrations may cause relatively large fluctuations in number fractions). Thus, distinguishing the effect of entrainment from measurement uncertainties/biases can be tricky.

In order to minimize the possible biases arising from minimization, the residual (Eq. 8) was calculated over the 80–200 nm size range.

c. *Our experience from similar measurements at the Jungfraujoch research station is that the diameter range across which $f_{act,DMPS}$ increases from 0 to 1 is much broader than can be explained with the heterogeneity of the aerosol in terms of mixing state/GF-PDF (the JFJ-aerosol is rather internally mixed). This indicates that the width of $f_{act,DMPS}$ is mainly driven by heterogeneity of $S_{c,eff}$ on small spatial scales due to e.g. turbulence. What does it look like in your case (the aerosol at Puijo is obviously much more externally mixed than that observed at the Jungfraujoch)? Can the shape of $f_{act,DMPS}(D_p)$ be explained with the external mixing alone? This question possibly goes beyond the main focus of this paper, but it might still be worth looking at it. You have the data at hand and could possibly produce a supplementary figure using representative examples).*

Response: One criteria for case selection in Sect. 3.4 (and Sect. 3.5) was that the $f_{act,HTDMA}$ managed to produce the size-dependence/slope similar to $f_{act,DMPS}$. Ideally (assuming that the GF-surfaces were well-predicted), this would indicate that the changes in hygroscopicity/mixing state were enough to explain the width of $f_{act,DMPS}$.

However, as pointed out in the revised manuscript, this wasn't always the case and thus, we can't exclude the possible influence of turbulent/heterogeneous $S_{c,eff}$. This is definitely an interesting topic but would require a much more comprehensive set of analysis to be addressed adequately.

d. *An alternative approach would be to fit something like a sigmoid curve into $f_{act,DMPS}(D_p)$ to obtain an effective activation cut-off diameter (half rise). Inserting this cut-off diameter and $\kappa_{avg}(D_p)$ into Köhler theory then provides $S_{c,eff}$ under the assumption of internal mixing. I would expect that these values are very similar to those obtained with your approach accounting for external mixture. If not, you should comment on the fact that proper treatment of mixing state is crucial for inferring $S_{c,eff}$ when dealing with clouds formed on externally mixed aerosol.*

Response: This is also a good idea. However, determination of cloud supersaturation is likely beyond the main scope of the current manuscript and will be examined more comprehensively in future studies.

e. *Did you define $f_{act,DMPS}(D_p)$?*

Response: The definition of $f_{act,DMPS}$ is added to the manuscript.

17. Comment: *P.6, l.26ff: First, this paragraph belongs above the paragraph describing how you infer $S_{c,eff}$, as this is still about predicting CCN number concentration from HTDMA data, if I got that right. Second, you may have to explain how you obtain $\kappa_{avg}(D_p)$.*

Response: We have decided to keep the order of these paragraphs as they are. The main idea here is that adjusting the S_c is an integral part of determining $N_{act,HTDMA}$, rather than an individual analysis. Another reason is that the obtained $S_{c,eff}$ values are later used in the internally mixed approach.

We have rephrased the paragraph describing the internal mixing approach to improve the language and clarity.

18. Comment: *Sect. 3.1: Some at least partially glaciated clouds wouldn't be surprising if ambient temperature was sometimes below zero (minimum was -9.7 °C).*

Response: The minimum temperature during cloud events was -5.8 °C. Although we do not have direct measurements on ice nuclei activity, our current perception is that glaciation plays a very minor role at these temperatures (at Puijo).

19. Comment: *Figure 1, bottom row: GF-PDFs shown here are normalized to unit area. I wonder whether it would be instructive to add an extra row (or replace the current bottom row) with a version in which you re-normalize the GF-PDFs as follows. For the total aerosol, multiply the GF-PDF that is already normalized to unit area with $dN_{tot}/dlogD_p(D_p)$. And equivalently for the interstitial aerosol. The area between the curves representing the total and interstitial GF-PDFs for equal size would then directly correspond to the activated particles. Furthermore, normalized in this manner, the bottom row of Figure 1 would then be are more close graphical representation of what you calculate with Equation 9. You could even add an extra row of panels that shows $f_{act,GF}$ for each diameter and GF-resolved, i.e. as a function of GF rather than integrated over a GF range.*

Response: Due to highly variable total/interstitial concentrations, averaging these kind of "non-normalized" GF distributions would result in very different looking distributions compared to what is presented in the current version of Fig. 1 (i.e., the averaged distributions would be largely biased towards the observations with high concentrations). To avoid any confusion, we've decided to keep the Fig. 1 as it is and include the suggested figure in the supplementary material. In this figure, shown are the median GF distributions and their 25th and 75th percentiles determined from hourly averaged HTDMA+DMPS observations.

20. Comment: *P.7, l.20: Was the shift of the more hygroscopic mode towards larger GF with increasing particles size less or more than what can be explained by the size dependence of the GF imposed by the Kelvin effect?*

Response: Typically, the κ values of more hygroscopic particles increased with particle size indicating that the Kelvin effect alone was not enough to explain the observed shift towards larger growth factors. This can be seen from Fig. 1 (see the attached figure below) showing the average κ-PDFs calculated over the whole measurement campaign. This figure is also included in the manuscript together with a brief explanation.

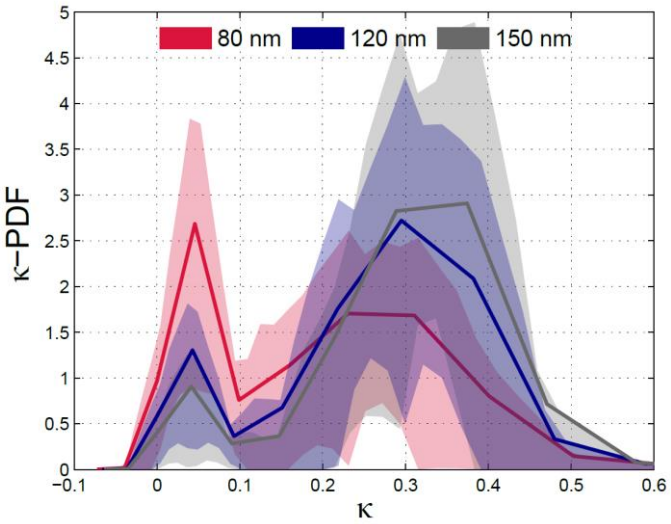

Fig. 1: Mean κ-PDFs of 80, 120 and 150 nm particles averaged over the whole campaign. The shaded areas represent the ranges between the 25th and 75th percentiles.

21. Comment: *P.7, l21ff: The observations by Laborde et al. (2013) in Paris revealed even a little more detail. There was very clear evidence that particles from fresh traffic emissions appeared mainly at GF≈1.0, whereas particles from wood burning appeared mainly at GF≈1.1, together forming the "nonhygroscopic" mode in the HTDMA. I have added this detailed remark because the GF-PDFs shown in the bottom row of your Figure 1 for particles with diameters of 120 nm and 150 nm seem to provide evidence that the cloud droplet active fraction differs slightly between GF≈1.0 and GF≈1.1. Could you confirm this or is this difference within uncertainty?*

Response: This is a good point. As we mentioned in our response to comment #2, the difference between the interstitial and total concentrations ("TOT-INT") could become negative if the activated fraction was low. When estimating the residual GF-PDFs, these values are first set to zeros, which leads to a strengthening of positive peaks when the distributions are normalized. Therefore, the difference between GF = 1 and GF = 1.1 is at least partially an artefact, rather than a real difference in activation efficiency. This is now explained in the manuscript.

22. **Comment:** *Equation 9: $N_{tot}(D_p)$ should be replaced by $dN_{tot}(D_p)/dlogD_p$, shouldn't it? And so for $N_{int}(D_p)$? – You define N_{tot} as: "…where N_{tot} and N_{int} are the total and interstitial number concentrations…". This rather rather sounds as if $N_{tot}(D_p)$ was representing a cumulative number concentration, which would be wrong in Equation 9 (as I understand the purpose of Equation 9).*
PS: you could of course also choose $dN_{tot}(D_p)/dD_p$ instead of $dN_{tot}(D_p)/dlogD_p$ as the factor in between those two eventually cancels out.
*Besides: I recommend adding another line to Equation 9, in which you rearrange it as follows: fact,GF1<GF<GF2(Dp, GF1, GF2)= (dNtot(Dp)/dlogDp * f tot,GF1<GF<GF2(Dp) – dNint(Dp)/dlogDp * f int,GF1<GF<GF2(Dp)) / dNtot(Dp)/dlogDp * f tot,GF1<GF<GF2(Dp) where $f_{tot,GF1<GF<GF2}(D_p)$ is the number fraction of particles (total aerosol) with dry diameter D_p and GF between GF1 and GF2 (and equivalent for the interstitial particles). This addition should help in understanding the meaning of Equation 9.*

Response: We have modified the equation as suggested.

23. **Comment:** *P.9, l.3ff: "The most interesting remark concerns the difference between the low and high hygroscopicity particles at 120 and 150 nm. While the activation efficiency of total aerosol and more hygroscopic particles increases with size, the less hygroscopic particle mode remains almost non-activated." – The "size dependence" mentioned in this statement is distracting from the main message. In my view Table 1 already captures the central and very nice results of your study, which is: "…., the cloud droplet activated fraction of the less hygroscopic particles is much smaller than that of the more hygroscopic particles of equal size…which confirms that cloud droplet activation critically depends on particle hygroscopicity for particle sizes for all sizes in the range of the droplet activation cut-off…." The very nice thing is that you showed this, which is expected based theory and hygroscopicity-resolved HTDMA-CCN closure studies, for the activation of atmospheric aerosols in atmospheric clouds. Personally I would focus on this, i.e. comparing less versus more hygroscopic at equal size, and address size dependence in the next paragraph.*

Response: This part of the manuscript has been re-written according to the updated results.

24. **Comment:** *P.9, l.11ff: "Here, the residual aerosol-properties were estimated indirectly by using the hourly averaged total and interstitial GF-PDFs and their actual number concentrations." – Which factors did you apply to the normalized GF-PDFs, $dN_{tot}(D_p)/dlogD_p$ and $dN_{int}(D_p)/dlogD_p$ for the total and interstitial inlets or did you revert the normalization factor of the GF-PDFs with the normalization factor that had been applied? I would believe that the former is the better choice, if the total and interstitial DMPS measurements are corrected such that they are identical for out of cloud measurements. However, this is just a subtlety.*

PS: Applying the number of counts of the HTDMA raw measurements would be "wrong" because the detection probability in the HTDMA is GF-dependent for a fixed dry size. However, again just a small but still systematic bias.

Response: In the original manuscript, the GF-PDFs were scaled by using the concentrations derived from HTDMA measurements. In the current version, we are instead using the DMPS derived concentrations. This now clarified in the manuscript.

25. **Comment:** *P.9, l.10-17: why do you not discuss the size dependence of the activated fractions of the more and of the less hygroscopic particles in this paragraph? There are good reasons for how they depend on size and why there is hardly any difference between total and interstitial inlet at the smallest covered size.*

    Response: We have added a couple of sentences regarding the observed size dependence.

26. **Comment:** *Figure 1: According the legend in the bottom row of Figure 1 the difference of the average GF between total and interstitial inlet is 0.04 for the two dry diameters 80 nm and 120 nm. However, the difference between total and interstitial seems to be much larger for 120 nm compared to 80 nm when looking at the bottom row of Figure 1. Please check carefully and adapt the figure and discussion on P.9 l.10-17 if needed*

    Response: Thank you for pointing this out. There was indeed a mistake in the legend values in the case of interstitial aerosol. The figure is updated with revised values and the discussion is adapted.

27. **Comment:** *P.9, l.18 ff: "To our knowledge, this is one of the very few studies characterizing the hygroscopic properties of different in-cloud aerosol populations." – there might exist some CCN based literature on this topic; you could check for authors like U. Pöschl and D. Rose. Concerning chemical composition: you could check for SP2-based studies by J. Schroder et al. This might potentially link in to the behaviour of the less-hygroscopic particles.*

    Response: We have added a reference to discussion paper by Rose et al. (2013).

28. **Comment:** *Figure 2 and associated discussion: Relevant analysis, however, somewhat incomplete. Equation 5 tells us that the three parameters S_c, κ and D_{50} are related to each other. Therefore, the relation between the three of them should be reflected in the analysis, figures and discussion. Some thoughts on this:*

    a. *The dependence of D_{50} on κ could be the result of cross-correlation rather than causality. You should confirm that κ and S_c are not correlated to make your result stronger. This is definitely required before you make the statement at the end of Section 3.3.*

    Response: No correlation was found between κ and $S_{c,eff}$ ($R^2 \sim 0.02$). This is now mentioned in the manuscript.

    b. *Color code: the most relevant information I seem to learn from the colour code is that the variability of κ is for the most part driven by the variability of the number fraction of less and more hygroscopic particles rather than the variability of the respective mean GFs of these two modes. Correct? This would be better seen from a scatter plot of κ versus $f_{GF<1.25}$.*

Response: This essentially true. According to simple linear correlation, the less hygroscopic fraction explained approximately 80% of the total variation in κ regardless of particle size. On the other hand, the less hygroscopic fraction is also linked to the position of the more hygroscopic mode ($R^2 \sim 0.3–0.4$), which makes the comparison a bit more complicated.

c. *Fit curve: the fit curve can be quantitatively interpreted, i.e. it provides you an estimate about the $S_{c,eff}$ "averaged" over the whole data set. Is this value consistent with your other analyses of $S_{c,eff}$? Caveat: Equation 5 is an approximation, which is likely not accurate for the rather low critical supersaturations you are dealing with.*

Response: This estimation is given in Sect. 3.4.

d. *I suggest you include multiple theoretical lines in Figure 2 that show D_{50} versus κ for different S_c (based on unbiased numerical solutions rather than the approximate Equation 5). These theoretical lines might possibly save you the trouble of including a fit curve. Additionally you should choose the $S_{c,eff}$ as colour scale for the data points (you can have multiple versions with different colour scales if you like to keep your old colour scale too). This will give you a more complete picture on the influence of κ, $S_{c,eff}$ and also "measurement noise" on the variability of D_{50}.*

Response: We have added theoretical lines for critical supersaturations of 0.10, 0.15, 0.20, 0.30, 0.40 and 0.50%. However, the suggested figure (attached below) is included in the supplementary material. The reason is that due to the discrepancies between the HTDMA and DMPS derived activation properties (highlighted in Sect. 3.4), some of the determined $s_{c,eff}$ values were most likely characterized by increased uncertainties.

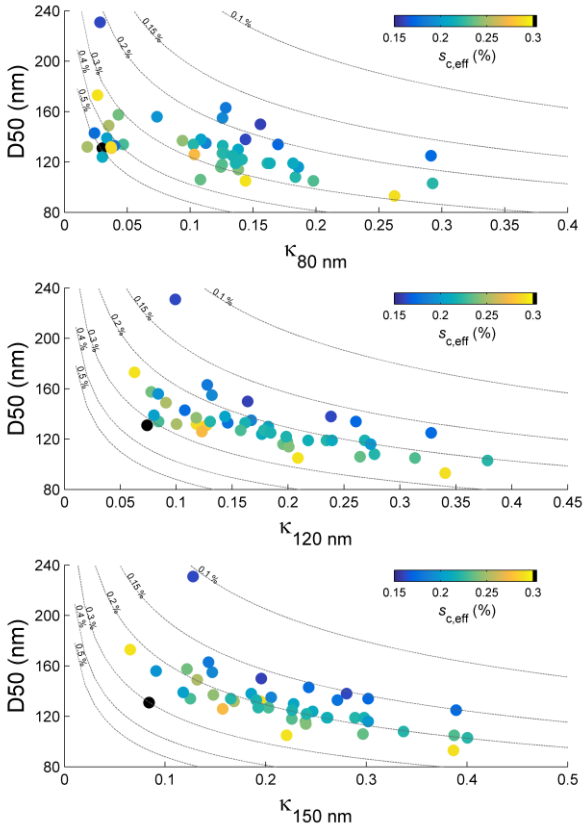

e. *You should also create a figure in which you swap the roles of κ and $S_{c,eff}$, i.e. you plot D_{50} vs $S_{c,eff}$ and choose κ_{avg} (I'd say for 120 nm or 150 nm or a value interpolated to the mean D50) as colour scale (theoretical lines should also be added). How does it compare with the figure suggested above?*

Response: This figure is also included in the supplementary material.

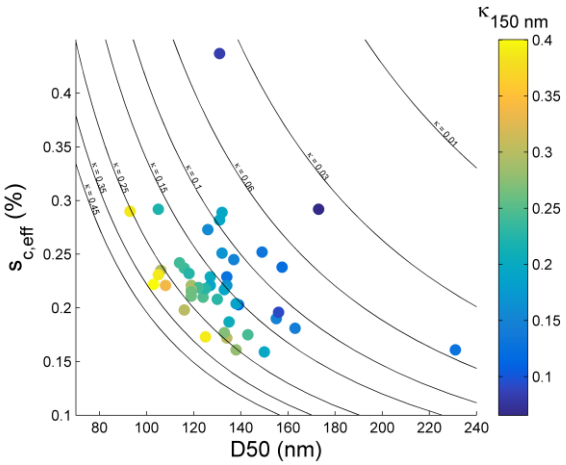

f. *The outlier in Figure 2: is it an outlier in the sense of "cannot be explained" or do you have independent evidence that the very high D_{50} could possibly be caused by exceptionally low supersaturation (you cannot use $S_{c,eff}$. to argue as $S_{c,eff}$ is inferred from D50)?*

Response: In this case, the D50 was most likely biased towards larger sizes due to the uncertainties arising from extremely low number concentrations (i.e., the activation curve wasn't perfectly smooth around ~170–240 nm).

29. **Comment:** *P.10, l.28-29: "…the estimated peak supersaturations… …they provide some valuable information about the in-cloud conditions…". – The droplet activation happens at the initial stages of cloud formation.*

Response: This paragraph is rephrased as "…about the conditions relevant to cloud droplet formation".

30. **Comment:** *Last paragraph of Section 3.4 (comparison of supersaturations with literature): Hammer et al. (2014) reported a systematic difference in observed peak supersaturations for the two prevalent wind directions, which could be explained by differences in the orographic forcing (steep vs gentle mountain slopes). What are the cloud formation mechanisms for the clouds probed at Puijo (and Pallas)? Are the lower peak supersaturations at those two sites possibly related to weaker orographic forcing compared to the Puy de Dôme and Jungfraujoch sites?*

Response: We are currently preparing a manuscript concentrating on the effect of updrafts on cloud properties at Puijo. The preliminary model results suggest that due to the reasonably low height of the Puijo hill and the fact that the measurement station is located on the top of a 75-metre tower, the terrain topography has a minor effect on the observed cloud properties. We have slightly widened the discussion regarding the results by Hammer et al. (2014).

31. **Comment:** *Figure 4 and associated discussion: The susceptibility of cloud droplet concentration to hygroscopicity can be quite asymmetric with respect to increase vs decrease of κ (see e.g. Figure 8 in Juranyi et al., 2010, or other studies that did similar sensitivity analyses for CCN number concentrations). Instead of just considering the case "no less hygroscopic particles at all" (higher κ), you could additionally consider the case "no more hygroscopic particles at all" (lower κ) for the sensitivity analysis presented in your Figure 4 and Table 2.*

*Jurányi, Z., Gysel, M., Weingartner, E., DeCarlo, P. F., Kammermann, L., and Baltensperger, U.: Measured and modelled cloud condensation nuclei number concentration at the high alpine site Jungfraujoch. Atmos. Chem. Phys., **10**, 7891-7906, doi:10.5194/acp-10-7891-2010, 2010. PS: further down in the manuscript it became clear why you specifically look at positive deviations. You could try to clarify this earlier.*

Response: Actually, we already performed this kind of an analysis when preparing the manuscript. In our opinion, however, including several scenarios provided only little added value considering the main message of our manuscript.

Anyhow, in case you're interested, please see the attached figure showing the results from simulations where the less hygroscopic GF modes were rescaled by a positive factor of 2.5 (i.e. the less hygroscopic fractions were increased by 150% → hygroscopicities decreased).

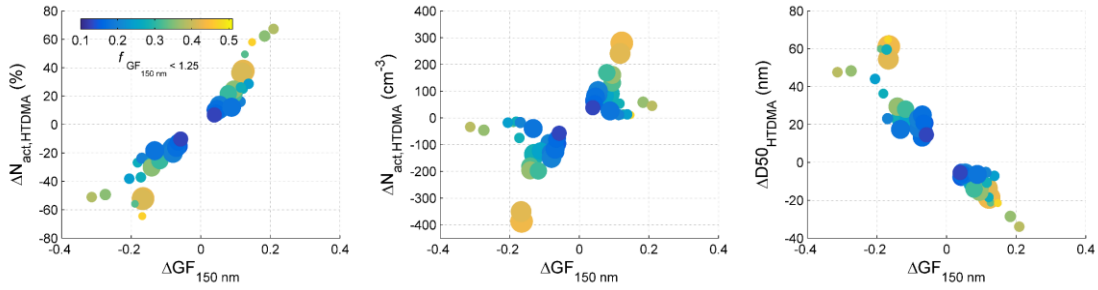

32. **Comment:** *Concerning difference of the activation behaviour of the two modes: As the aerosol at Puijo appears to have two rather well separated hygroscopicity modes, and since you prove that this directly affects the cloud droplet formation ability, you could quantify the expected difference of activation cut-off diameter for these two modes, if you like. One option would be the following: from "every" HTDMA measurement you can infer $S_{c,eff}$, $\kappa_{avg,GF<1.25}$ and κavg,GF>1.25. This allows to infer D50,GF<1.25 and D50,GF>1.25. Plotting D50,GF<1.25 and D50,GF>1.25 versus $S_{c,eff}$ then gives a fair idea of the activation cut-off diameter of the two modes, which is for example relevant for the threshold size down to which the particles in either mode can undergo cloud processing under the conditions in clouds at Puijo. (The only thing you would have to think about is how to deal with the diameter depends of hygroscopicity.)*

Response: A relevant analysis but most preferably to be included in future studies.

33. **Comment:** *There is another potentially interesting question you could look at if you like: while assuming an internally mixed aerosol can provide very good estimates of the total CCN number concentration, if properly done, it will not give an accurate answer concerning the respective contributions of the background aerosol and local/regional emissions to CCN number (with the picture in mind that the less hygroscopic mode is of local/regional origin). Based on your data set you could make at least a crude estimate of how the number fraction of local/regional particles compares between total aerosol and those particles that formed cloud droplets (pulling the idea of the previous comment even a little further). Or in other words: your data set seems to imply that most particles of local/regional origin have to undergo quite some atmospheric aging processes until they start participating in cloud droplet formation, doesn't it?*

    Response: This is also a very good idea and well-linked to our ongoing work concentrating on the influence of nearby pollution sources.

34. **Comment:** *l.26-27: "Understandably, by suppressing the size-dependent variations in chemical composition, the activation curves become steeper and the D50s decrease." – This is unclear. You only present data from a single size, so how can size dependence be suppressed? To my understanding the D50s decrease because you make the particles more hygroscopic! Please clarify how you mean this.*

    Response: The idea here is that neglecting the effect of less hygroscopic particles suppresses the size dependence of hygroscopic growth factors (that is, the average GFs increase much more clearly with particle size when the less hygroscopic mode in included – please see Table 2).

    As we are not changing the effective peak supersaturation, the activation starts to occur approximately at same sizes in both scenarios (original mixing state vs. high hygroscopicity assumption). However, as the particles become more hygroscopic the shape of the activation curves changes, i.e. the curves become steeper, which decreases the D50s. We have tried to use more precise wording here.

Technical corrections:

35. **Comment:** *P.7, l24: In the context of HTDMA measurements I would speak of "non-hygroscopic" particles for GF=1.0 rather than hydrophobic. I'd rather use the latter term in the context of measurements that are sensitive to "wettability", i.e. adsorption or contact angle or similar.*

    Response: Corrected as suggested

In-cloud measurements highlight the role of aerosol hygroscopicity in cloud droplet formation

Olli Väisänen[1], Antti Ruuskanen[2], Arttu Ylisirniö[1], Pasi Miettinen[1], Harri Portin[3], Liqing Hao[1], Ari Leskinen[1,2], Mika Komppula[2], Sami Romakkaniemi[2], Kari E. J. Lehtinen[1,2], Annele Virtanen[1]

[1]University of Eastern Finland, Department of Applied Physics, P.O. Box 1627, 70211 Kuopio, Finland
[2]Finnish Meteorological Institute, P.O. Box 1627, 70211 Kuopio, Finland
[3]Helsinki Region Environmental Services Authority, P.O. Box 100, 00066 HSY, Finland

Correspondence to: ~~A.~~Annele Virtanen (annele.virtanen@uef.fi)

Abstract. The relationship between aerosol hygroscopicity and cloud droplet activation was studied at the Puijo measurement station in Kuopio, Finland, during the autumn 2014. The hygroscopic growth of 80, 120 and 150 nm particles was measured at 90~~–~~% relative humidity with a hygroscopic tandem differential mobility analyzer. Typically, the growth factor (GF) distributions appeared bimodal with clearly distinguishable peaks around 1.0–1.1 and 1.4–1.6. However, the relative contribution of the two modes appeared highly variable reflecting the ~~varying~~probable presence of fresh anthropogenic particle emissions. The hygroscopicity-dependent activation properties were estimated in a case study comprising ~~three~~four separate cloud events with varying characteristics. At 120 and 150 nm, the activation efficiencies within the low- and high-GF modes varied between 0~~–0.33~~%–34% and ~~0.66–0.86,~~57%–83%, respectively, indicating that the less hygroscopic particles remained ~~almost~~mostly non-activated, whereas the more hygroscopic mode was predominantly scavenged into cloud droplets. By modifying the measured GF distributions, it was estimated how the cloud droplet concentrations would change if all the particles belonged to the more hygroscopic group. According to ~~the~~ κ-Köhler simulations, the cloud droplet concentrations increased up to 70~~ % with increasing hygroscopicity~~% when the possible feedback effects on effective peak supersaturation (between 0.16% and 0.29%) were assumed negligible. This is an indirect but clear illustration of the sensitivity of cloud formation to aerosol chemical composition.

1 Introduction

Atmospheric aerosols play a key role in the global climate system. They can affect the Earth's radiation balance either directly by scattering and absorbing the solar radiation, or indirectly, via clouds. Despite their relatively long-known influence pathways, atmospheric aerosols and especially their interactions with clouds, are still recognized as the most important source of uncertainty in the estimates of radiative forcing over the industrial period (IPCC, 2013). Although the climatic sensitivity and clouds are linked via numerous feedback mechanisms, one fundamental key towards a diminished uncertainty is to understand the factors controlling the particle's ability to act as cloud condensation nuclei (CCN).

The particles' ability to activate into cloud droplets ~~under~~at a certain ~~meteorological conditions~~level of supersaturation depends on their size and chemical composition. The role of particle size is already quite well identified and it's commonly considered as the most important factor. For example, according to the early model calculations by Junge and McLaren (1971) and measurements by Fitzgerald (1973), the shape of the CCN spectrum was predominantly determined by the initial particle size distribution, and compositional variations became significant only when the aerosol was highly insoluble. More recently, Dusek et al. (2006) estimated that the changes in aerosol size distribution explained over 80-% of the observed variance in CCN concentration. Similarly, Ervens et al. (2007) stated that the CCN predictions were the most sensitive to variations in particle size distribution and supersaturation.

Considering the great climatological uncertainty related to aerosol-cloud interactions, such a straightforward relationship between aerosol size distributions and CCN spectra could substantially improve the estimates of the aerosol indirect radiative forcing. However, as Hudson (2007) stated, the estimation by Dusek et al. (2006) was based on rather small variation in chemical composition, which may have led to considerable underestimation of its role in cloud droplet activation. In addition, Quinn et al. (2008) parametrized the aerosol chemical composition by using the mass fraction of hydrocarbon-like organic aerosol (HOA) and combined the results with CCN activity measurements. The results indicated that the uncertainty between the measured and estimated CCN concentrations was up to 50-% when the variations in HOA were neglected.

During the last few decades, a lot of effort has been put into CCN closure studies, i.e. determination of CCN concentration by means of size and composition related properties (Broekhuizen et al., 2006; Conant et al., 2004; Ervens et al., 2007; Fountoukis et al., 2007). CCN closure studies allow to assess the importance of different parameters on cloud droplet activation and therefore, they are an important tool towards a sufficient understanding of the link between atmospheric aerosols and cloud processes. One specific method includes the determination of CCN ~~spectrum~~spectra by means of hygroscopicity measurements. Under subsaturated conditions (i.e. relative humidity (RH) < 100–%), aerosol hygroscopicity can be characterized by using a parameter called hygroscopic growth factor

$$\mathrm{GF}(\mathrm{RH}, D_\mathrm{p}) = \frac{D_\mathrm{wet}(\mathrm{RH}, D_\mathrm{p})}{D_\mathrm{p}}, \quad (1)$$

where D_wet is the wet particle diameter at a certain RH and D_p is the corresponding dry diameter. In principle, GFs reflect the aerosol chemical composition. Pure inorganic salts such as sodium chloride (NaCl) and ammonium sulfate ($(NH_4)_2SO_4$) are usually associated with elevated growth factors (GF > 1.60 at RH = 90-%), whereas some other species appear clearly less hygroscopic (McFiggans et al., 2006). For example, fresh mineral dust and pure black carbon are almost hydrophobic with typical GFs below 1.05 (Vlasenko et al., 2005; Weingartner et al., 1997; Liu et al., 2013). In atmospheric conditions, the average GFs usually vary between 1.0 and 1.8, and the GF distributions may consist of several independent modes originating from various sources of particulate matter (Ferron et al., 2005, Fors et al., 2011; Sjogren et al., 2008; Liu et al., 2011; McFiggans et al., 2006).

In order to better understand the relationship between cloud droplet activation, aerosol chemical composition and hygroscopicity, we organized an intensive measurement campaign at the Puijo measurement station in Kuopio, Eastern Finland, during the autumn 2014 (Puijo Cloud Experiment 2014). Along with the Global Atmospheric Watch (GAW) stations such as Pallas, Finland (Komppula et al., 2005), Jungfraujoch, Switzerland (Sjogren et al., 2008) and Puy-de-Dôme, France (Asmi et al., 2012), the Puijo station is one of the few measurement sites, where long-term continuous in situ measurements on aerosol-cloud interactions are being carried out. Therefore, it provides an established base for detailed aerosol and cloud studies. Utilizing the conducted in-cloud measurements, this paper aims to identify the hygroscopicity-dependent activation properties of a cloud-forming aerosol population and study the effects of varying chemical composition on cloud droplet formation.

2 Methods

2.1 Measurement site

The measurement campaign took place at the Puijo SMEAR IV station in Kuopio, Finland (around 340 km to NE from Helsinki) between 17 September and 4 November 2014. The measurement station is located at the top of the Puijo observation tower (62°54'34'' N, 27°39'19'' E) approximately 224 m above the surrounding lake level (Leskinen et al., 2009; Ahmad et al., 2013; Portin et al., 2014). The station was established in 2005 and since then it has provided continuous data on aerosol and cloud droplet size distributions, aerosol optical properties, atmospheric trace constituents and ~~different~~various weather parameters. Due to the diverse surroundings, the measurement site can be characterized as a semi-urban environment. The eastern side of the tower (0–215°) includes several local pollution sources such as a paper mill in the northeast, the city center in the southeast, a heating plant in the south and the two main roads in south–north direction, as well as residential areas with occasional domestic biomass combustion. By contrast, the western sector (215–360°) has no important local sources besides the relatively small residential areas. For more detailed overview of the station and local pollution sources, see Leskinen et al. (2012) and Portin et al. (2014).

2.2 Weather data and cloud events

Temperature, visibility, wind speed, wind direction, precipitation, air pressure and relative humidity were measured continuously during the campaign. Visibility and precipitation were measured with a Vaisala FD12P weather sensor, wind speed and direction with an ultrasonic two-dimensional anemometer (Thies UA2D), and temperature and relative humidity with a Vaisala HMT337 temperature and humidity transmitter. Based on meteorological conditions, the measurement period was divided into cloudy and cloud-free sub-periods. Cloud events were defined as continuous periods (duration more than 1 h) with visibility below 200 m. For cloud-free conditions, the lower visibility limit was set to 8000 m in order to avoid the biasing effects of non-uniform clouds and fog. In addition, the observed events were classified as rainy if the average rain

intensity exceeded 0.2 mm h^{-1}. However, these cases were omitted from the analyses, since precipitation removes both activated and non-activated particles from the atmosphere causing a possible source of error for the measurement data.

2.3 Twin inlet system and size distribution measurements

During the campaign, we utilized a custom made twin inlet system (Portin et al., 2014) consisting of two separate sample lines in order to measure total and non-activated (interstitial) particles separately. The total air inlet had an approximate cut-off diameter of 40 µm and the sample line was heated to 30–40 °C. Due to the heating, liquid water was evaporated from the droplets and residual particles were formed. Thus, when the top of the tower was inside a cloud, the total flow contained both the residual and interstitial particles. Meanwhile, the interstitial sample line was equipped with a $PM_{1.0}$ impactor (lower cut-off limit of 1 µm) to prevent the cloud droplets from entering the sampling system. During cloud-free conditions, both of the inlets sampled the same aerosol population.

Aerosol size distributions from 3 to 800 nm were measured with a twin differential mobility particle sizer (twin-DMPS). ~~Two~~In this setup, two independent DMPSs measured the particle diameters from 3 to 53 nm and from 30 up to 800 nm with aerosol/sheath flow ratios of 1.4:23 and 1:5.5, respectively. The ~~instrument was~~instruments were attached to the twin inlet system with an automated valve, which was operated to switch between the sampling lines in 6-minute intervals. Consequently, the total measurement time for total and interstitial population was 12 minutes, assuming that the aerosol was not changing during the cycle. Full data inversion was applied to the raw data~~,~~ including corrections for sampling losses, multiple charging probabilities, instrumental transfer functions and particle counting efficiencies~~.~~ as recommended by Wiedensohler et al. (2012).

2.4 HTDMA experiments

Aerosol hygroscopicity under subsaturated conditions was measured with a hygroscopic tandem differential mobility analyzer (HTDMA, Table S1). Briefly, HTDMA consists of two differential mobility analyzers (DMA) and a humidifier. The first DMA (DMA1) selects the dry size of interest and the second DMA (DMA2) coupled with a condensation particle counter (CPC) measures the resulting size distribution, after the nearly monodisperse aerosol sample has been exposed to certain RH. During the campaign, the initial dry sizes were 80, 120 and 150 nm and the RH inside the DMA2 (RH_{DMA2}) was adjusted to ~90~~-~~%. Both of the DMAs were 28 cm long Vienna type DMAs (Winklmayr et al., 1991) operated with flow ratios of 1:6, and the RH control of the sheath air inside ~~the~~ DMA2 was achieved by using a closed-loop circulation. The residence time ~~between~~inside the aerosol humidifier ~~and particle sizing~~was approximately 0.2 s, after which the particles spent ~2 s in elevated RH before entering the DMA2~~ was ~2 s, and the~~. The propagated instrumental uncertainty associated with the measured GFs was approximately ±4.5~~-~~%.

The ~~instrument~~HTDMA was attached to the ~~changing~~twin inlet system for a 4-week period (26 September – 20 October; hereafter referred as a twin inlet period) in the middle of the campaign. Otherwise, total aerosol was being measured continuously. During the twin inlet period, an external valve system switched between the two sampling lines in 24~~–~~minute

intervals. Therefore, the duration of individual size scans was adjusted so that the whole measurement cycle with three initial dry sizes was performed twice between each line change. However, some of the data points had to be removed afterwards because the line change had occurred during an ongoing size scan. In the case of continuous total line measurements, each size scan took 5 minutes.

The average hygroscopic growth factors and their probability density functions (GF-PDF) were evaluated using the TDMAinv inversion toolkit (Gysel et al., 2009). The procedure calculates the broadening factor of the instrumental transfer function from ~~the~~ dry size measurements and then describes the inverted GF-PDFs as piecewise linear functions. For this purpose, dry size scans with ammonium sulfate particles were performed at low RH before and during the campaign. The inversion algorithm was operated to solve the GF-PDFs with a resolution of $\Delta GF = 0.10$ and only the size scans with average RH_{DMA2} between 88 % and 92~~-~~% were taken into account in the analysis. In addition these data points were corrected to the 90~~-~~% target RH by using the built-in γ-model within the inversion toolkit. Briefly, γ-correction adjusts the measured growth factors to the desired RH by applying ~~the~~a parametrization $GF = (1\text{-}RH)^{-\gamma}$, where γ is first calculated from the original measurement data and then substituted backwards to obtain the RH corrected ~~growth factor~~GF.

2.5 Derivation of $N_{act,HTDMA}$

According to the Köhler theory (Köhler, 1936), the equilibrium saturation ratio, ~~S_e~~S_{eq}, over a liquid droplet can be calculated by

$$\text{~~}S_e\text{~~}S_{eq} = a_w \exp\left(\frac{4M_w\sigma}{RT\rho_w D_{wet}}\right), \quad (2)$$

where a_w is the water activity, M_w the molar weight of water, σ the surface tension (here, assumed to be that of water, 0.072 J m^{-2}), R the universal gas constant, T the ambient temperature and ρ_w the density of water. In order to relate the measured growth factors to water activities, we used the κ-Köhler model described by Petters and Kreidenweis (2007). With κ-Köhler model, the water activity can be parametrized as

$$\frac{1}{a_w} = 1 + \kappa\frac{V_{sp}}{V_w}, \quad (3)$$

where ~~V_s~~V_p and V_w are the ~~soluble~~dry particle and water volumes, and κ is the hygroscopicity parameter determined as below:

$$\kappa(GF, D_p, RH) = \frac{(GF^3-1)\exp\left(\frac{4M_w\sigma}{RT\rho_w D_p GF}\right)}{RH} - GF^3 + 1. \quad (4)$$

Alternatively, the relationship between κ and critical saturation ratio, S_c, i.e. the maximum of the Köhler curve (Eq. 2), can be ~~related to S_e~~approximated by

$$\kappa(D_p, S_c) = \frac{4A^3}{27 D_p^3 \ln^2 S_c}, \quad (5)$$

where $A = 4M_w\sigma/RT\rho_w$. Thus, by combining the Eqs. (4) and (5) and by assuming a certain value for S_c, it is possible to estimate the critical growth factor, GF_c, i.e. the required growth factor for particles with dry size D_p to become activated at the given supersaturation. Thereafter, the size-resolved activation efficiency $f_{act,HTDMA}$ can be calculated according to

$$f_{act,HTDMA}(D_p, S_c) = \int_{GF_c(D_p,S_c)}^{\infty} \text{GF-PDF}(GF, D_p) dGF. \quad (6)$$

Furthermore, the available CCN concentration can ~~now~~ be obtained by weighting the measured particle size distribution with the activation efficiency and by integrating over the whole size range:

$$N_{act,HTDMA}(S_c) = \int_{-\infty}^{\infty} f_{act,HTDMA}(D_p, S_c) \frac{dN_{tot}}{d \log D_p} d \log D_p. \quad (7)$$

In order to solve the preceding equation, the GF-PDFs determined for D_p = 80, 120 and 150 nm were linearly interpolated to cover the whole size range of interest. This was done by interpolating the GF-PDFs over the measurement range (80–150 nm) and then extrapolating up to 200 nm. In addition, the 80 and 200 nm GF-PDFs were assumed to be representative for particles smaller than 80 nm and larger than 200 nm, respectively.

The procedure follows the principles described ~~by~~ previously by e.g. Kammermann et al. (2010b) and Fors et al. (2011), except that here we did not have an independent HTDMA data point around 200–250 nm. Therefore, extrapolation ~~to~~towards larger sizes is also the main source of uncertainty~~. At larger particle sizes,~~ as underestimation of aerosol hygroscopicity could possibly lead to underestimation of $f_{act,HTDMA}$ and vice versa. ~~Nonetheless, it has to be noted that above 200 nm, hygroscopicity is quite rarely a limiting factor and the most crucial activation characteristics are dependent on particle properties between the ~80 nm and ~200 nm sizes.~~ Secondly, the method assumes that the subsaturated hygroscopicities are representative for supersaturated conditions. Such an assumption is not always totally valid and discrepancies between the two saturation regimes have been reported based on laboratory and field experiments (Good et al. 2010; Hersey et al., 2014; Jaatinen et al., 2014; Pajunoja et al. 2015). Typically, the subsaturated hygroscopicities can appear somewhat lower than the supersaturated ones, which may result in underestimation of CCN concentration at a fixed supersaturation. On the other hand, for example Jurányi et al. (2013) found a very good closure between the sub- and supersaturated regimes for an externally mixed urban aerosol in Paris, France.

In order to estimate the cloud droplet concentration in atmospherically relevant conditions, the effective peak supersaturation, ~~s_{eff}~~$S_{c,eff}$ (where ~~$s_{eff} = S_{eff}$~~$S_{c,eff} = S_{c,eff} - 1$), was approximated by minimizing the difference between the measured ~~(DMPS)~~ and estimated ~~(HTDMA)~~ activation curves, i.e. by minimizing the norm

$$||R(S_c)|| = \sqrt{\sum_i \left[f_{act,HTDMA}(D_{p,i}, S_c) - f_{act,DMPS}(D_{p,i})\right]^2}, \quad (8)$$

where $D_{p,i}$ was limited to vary from 80 to 200 nm. It's, and the DMPS derived activation efficiency, $f_{act,DMPS}$, was determined by means of total and interstitial particle size distributions as follows:

$$f_{act,DMPS}(D_p) = \frac{\frac{dN_{tot}}{d\log D_p}(D_p) - \frac{dN_{int}}{d\log D_p}(D_p)}{\frac{dN_{tot}}{d\log D_p}(D_p)}. \quad (9)$$

In principle, the effective peak supersaturation can be described as the maximum supersaturation that the particles experience for an adequate time to form stable cloud droplets (Hammer et al. 2014). It's also important to point out that this kind of approach masks the potential discrepancies between the two saturation regimes, and underestimation of supersaturated hygroscopicity willwould eventually lead to positive bias in $s_{eff}$$S_{c,eff}$.

In addition to the "externally mixed approach" described above, the cloud droplet concentrations were estimated by representingunder an assumption that the ambient aerosol was completely internally mixed. In this approach, the interpolated GF surfaces in terms of size-averagedwere used to calculate the average hygroscopicity parametersparameter κ_{avg}(D_p). This (Eq. 4) for each dry size. These values were then compared to critical κ values approximated by using the Eq. (5) and the previously determined $S_{c,eff}$. Furthermore, depending on whether the κ_{avg} was higher or lower than the respective critical value, the activation efficiency was assumed to be either 1 or 0, respectively. Therefore, this kind of internally mixed approach resultsresulted in activation efficiency curves resembling a step function instead of S-shaped curves obtained fromby means of full GF-PDFs. More precisely, the size dependent activation efficiency equals either 0 or 1 depending on whether the κ_{avg}(D_p) is lower or higher than the critical κ(D_p,S_{eff}) calculated by Eq. (5).

3 Results and discussion

3.1 Weather parameters and cloud events

During the campaign, the hourly averaged ambient temperatures varied between -9.7 °C and 15.3 °C, with sub-zero temperatures occurring mostly during the latter half of the measurement period. Due to the diurnal temperature variations, relative humidity usually reached its daily maxima during the nighttime and early morning hours. Therefore, most of the cloud formation events also occurred within these time periods. Generally, the wind speeds exhibited a diurnal variation similar to ambient RH with slightly increased velocities during the nighttime. The wind was blowing from southwestern directions (180–270°) approximately 39-% of time, and during cloud events, this fraction was even higher, roughly 50-%. Altogether, the tower was inside a cloud approximately 10-% of time, which is somewhat less compared to typical autumn conditions at Puijo (Portin et al., 2009). In total, 15 non-precipitative cloud events were observed during the campaign, providing up to 47 cloud event hours.

3.2 Hygroscopicity at Puijo

Figure 1 shows the average GFs and GF-PDFs observed at Puijo during the campaign period. Overall, the measured GFs varied between ~1 and ~1.7 reaching the campaign averages (± 1 standard deviation) of 1.30 ± 0.11 (80 nm), 1.42 ± 0.10 (120 nm) and 1.47 ± 0.10 (150 nm). A closer look at the GF-PDFs indicates that there are two main factors affecting the observed size dependence. In general, the GF-PDFs ~~appeared~~appear bimodal with clearly distinguishable peaks around 1.0–1.1 and 1.4–1.6. However, the number fraction of less hygroscopic particles ($f_{GF<1.25}$) decreases with increasing particle size, and at the same time, the more hygroscopic mode tends to shift slightly towards larger growth factors. A similar shift is also apparent in Fig. 2 where the average hygroscopicity distributions are plotted as κ-PDFs. Furthermore, this indicates that the transition towards higher GFs can be attributed both to Kelvin effect as well as changes in chemical composition.

According to a wind sector analysis (see supplementary material for further details), the polluted sector was characterized by higher $f_{GF<1.25}$ than the clean one, but on the other hand, the more hygroscopic mode shifted towards higher GFs suppressing the differences in average GFs. Tiitta et al. (2010) studied the particulate roadside emissions in Kuopio and observed an elevated ~~hydrophobic~~non-hygroscopic particle mode ($D_p \leq 50$ nm) originating from fresh exhaust emissions. A similar observation was also made by Laborde et al. (2013) in Paris with particle sizes up to 265 nm. Against this background, it is probable that the less hygroscopic fraction observed at Puijo is also linked to the traffic and other anthropogenic ~~particle emissions~~sources of organic aerosol.

Minor differences can be seen also in the GF-PDFs between cloudy and cloud-free conditions (Fig. 1). The fraction of more hygroscopic particles is slightly enhanced during ~~the~~ cloud-free conditions, resulting in higher average GFs. This can be due to the limited time scale of cloud events and varying contribution of local pollution, together with possibility for in-cloud processing and precipitation scavenging. However, for example Henning et al. (2014) and Zelenyuk et al. (2010) reported a cloud-induced sulfate enrichment in the particle phase, which should eventually result in increasing hygroscopicity. One may also note that the in-cloud distributions measured during the ~~changing~~twin inlet period differ considerably from the campaign averages with substantially stronger contribution of $f_{GF<1.25}$ at D_p = 120 and 150 nm. Again, the most probable explanation is the enhanced presence of local pollution ~~resulting from~~due to more frequent ~~eastern~~easterly winds.

~~Analytical~~As indicated above, the analytical division between the ~~low~~less and ~~high hygroscopicity~~more hygroscopic particles was done by using a GF limit of 1.25. The value represents ~~the~~a common midpoint between the two GF modes and it has been used in several preceding studies (e.g. Kammermann et al., 2010a; Jurányi et al., 2013; Portin et al., 2014). Averaged over the whole campaign, the size-dependent less hygroscopic fractions were 0.44 ± 0.25 (80 nm), 0.22 ± 0.17 (120 nm) and 0.15 ± 0.14 (150 nm). Together with the ~~observed~~average GF-PDFs, these values are comparable to ~~the average~~ hygroscopicities ~~obtained~~observed at a back-ground site in southern Sweden (Fors et al., 2011). However, as seen during the ~~changing~~twin inlet period, our site experienced reasonably strong variation in less hygroscopic fraction with $f_{GF<1.25}$ regularly reaching the levels of urban conditions (McFiggans et al., 2006). For example during the observed cloud hours, the average $f_{GF<1.25}$ ranged from 0 up to 0.~~68~~62 at D_p = 150 nm. By comparison, Jurányi et al. (2013) studied the aerosol mixing state in Paris, France and reported

typical values varying between ~0.20 and ~0.60 at D_p = 165 nm. In addition, Ferron et al. (2005) observed that in urban and semi-urban conditions, the non-hygroscopic mode could be dominant at particle sizes up to 250 nm, especially during the autumn and winter seasons.

3.3 Hygroscopic properties of total, interstitial and residual aerosol

The GF-dependent activation efficiencies ($f_{act,GF}$) were ~~calculated~~derived from the measured GF-PDFs according to

~~$$f_{act}(D_p, GF_1, GF_2) = \frac{\int_{GF_1}^{GF_2}[N_{tot}(D_p)\times GF\text{-}PDF_{tot}(GF,D_p) - N_{int}(D_p)\times GF\text{-}PDF_{int}(GF,D_p)]\,dGF}{\int_{GF_1}^{GF_2} N_{tot}(D_p)\times GF\text{-}PDF_{tot}(GF,D_p)\,dGF}, \quad (9)$$~~

$$f_{\mathrm{act,GF_1<GF<GF_2}}(D_\mathrm{p}) = \frac{\frac{dN_\mathrm{tot}}{d\log D_\mathrm{p}}(D_\mathrm{p})\times f_{\mathrm{tot,GF_1<GF<GF_2}}(D_\mathrm{p}) - \frac{dN_\mathrm{int}}{d\log D_\mathrm{p}}(D_\mathrm{p})\times f_{\mathrm{int,GF_1<GF<GF_2}}(D_\mathrm{p})}{\frac{dN_\mathrm{tot}}{d\log D_\mathrm{p}}(D_\mathrm{p})\times f_{\mathrm{tot,GF_1<GF<GF_2}}(D_\mathrm{p})}, \quad (10)$$

where ~~N_{tot}~~ ~~$f_{tot,GF1<GF<GF2}$~~ and ~~N_{int}~~ ~~are~~ $f_{int,GF1<GF<GF2}$ were the total and interstitial number ~~concentrations~~fractions of particles with dry size D_p and GF between GF_1 and GF_2 ~~specify the applied GF range~~. The average activation efficiencies were calculated separately for each cloud event and for three different GF regimes (GF ≥ 0.80, 0.80 ≤ GF < 1.25 and GF ≥ 1.25). Here it should be noted that the activation efficiencies can appear negative if the averaged interstitial concentrations are higher than the corresponding total values. This can be the case especially within the less hygroscopic regime where the activated fractions are generally low. In such cases, the negative activation efficiencies are reported as zeros and treated as such when calculating the total activated fractions ($f_{act,GF≥0.80}$). Thus, the resulting $f_{act,GF≥0.80}$ values can be slightly different from those derived solely from DMPS measurements.

~~For comparison purposes, the~~A total ~~activated fractions were also determined from size distribution measurements. Typically, the activation efficiencies calculated by Eq. (9) ($f_{act,GF≥0.80}$) appeared somewhat larger than the DMPS derived values ($f_{act,DMPS}$). One possible explanation is the relatively~~ of nine cloud events were observed during the twin inlet period. Due to the reasonably low time resolution of ~~the~~ HTDMA size scans~~, which can lead to biased results if the changes in the air masses are not captured adequately by both of the sample lines. Therefore, we only present the results from three~~ and slow alteration between the two sampling lines, data with good coverage and reasonable agreement between $f_{act,GF>0.80}$ and $f_{act,DMPS}$ were available for four separate cloud events~~ with reasonably good agreement between the two methods.~~. These ~~three cloud events~~cases are summarized in Table 1. Because of the low activation efficiency of ultrafine particles, the ~~data is~~ activation parameters are presented only for 120 ~~nm~~ and 150 nm sizes.

The duration of the selected cloud ~~cases~~events varied from 1 h ~~20~~31 min (event #2) to 4 h 25 min ~~with event #1 being the shortest and (~~event #~~3 the longest. The cloud event #1 was characterized by western winds blowing across the clean sector. By contrast, the wind was blowing from the northeast and southeast during the cloud events #2 and #3, respectively. Some differences can be seen also in the hygroscopic characteristics. Event #2 was characterized by relatively small fraction of less~~

~~hygroscopic particles and the more hygroscopic mode was shifted towards larger GFs. Conversely,~~4). Cloud event #1 had ~~an elevated $f_{GF<1.25}$ and also the more hygroscopic mode appeared the least hygroscopic out of all three cases.~~

~~The most interesting remark concerns the difference between the low and high hygroscopicity particles at 120 and 150 nm. While the activation efficiency of total aerosol and more hygroscopic particles increases with size, the less hygroscopic~~ the highest particle ~~mode remains almost non-activated. As an exception, part of the less hygroscopic 150 nm particles seem~~and cloud droplet number concentrations, up to ~~have activated into cloud droplets~~2935 cm^{-3} and 781 cm^{-3}, respectively, whereas much lower values were observed during the latter events. For example during the cloud event #4, the particle and cloud droplet concentrations were down to 792 cm^{-3} and 69 cm^{-3}, respectively. These four cloud events were also characterized by very different wind patterns. Event #2 was influenced by westerly winds blowing across the clean sector. By contrast, the wind was from the northeast during cloud event ~~#1. However, this is only due to the reasonably large fraction of particles around GF =~~ 3 and from the southeast during the cloud ~~. Also, since this "intermediate" GF mode became visible at the end of the cloud~~ event~~, it's slightly uncertain if it~~ #4. Furthermore, event #1 was ~~present~~dominated by southwesterly winds blowing across the transition region between the clean and polluted sectors.

The most interesting remark, however, concerns the different activated fractions within the two GF modes. At D_p = 120 nm, the activation efficiencies of less hygroscopic particles varied from 0% to 4%, whereas the values for more hygroscopic particles were much higher (between 57% and 70%). A similar trend was observed also ~~during the preceding interstitial measurements. If this wasn't~~at D_p = 150 nm, with corresponding intervals of 0%–34% and 78%–83%, respectively.

One may also note that the hygroscopicity-dependent activation efficiencies increased with particle size. In the case~~, the reported value~~ of more hygroscopic particles, this was most likely attributed to Kelvin effect and small increments in respective hygroscopicities. Besides, the cloud events #2 and #4 were characterized by somewhat increased $f_{act,GF<1.25}$ ~~= 0.33 might be overestimated~~values at D_p = 150 nm. Although it is possible that part of these less hygroscopic particles were scavenged into cloud droplets, it's good to note that these cases were also characterized by notably low particle concentrations which may have led to increased uncertainties in activated fractions.

The difference between the activated and non-activated particles is also illustrated in Fig. 1 (lower panel) where the average GFs and GF-PDFs are presented separately for total, interstitial and residual aerosol populations. Here, the residual aerosol properties were estimated indirectly by using the hourly averaged total and interstitial GF-PDFs and ~~their actual number~~the respective ambient particle concentrations~~.~~ as follows:

$$c_{res}(GF, D_p) = \frac{dN_{tot}}{d\log D_p}(D_p) \times \text{GF-PDF}_{tot}(GF, D_p) - \frac{dN_{int}}{d\log D_p}(D_p) \times \text{GF-PDF}_{int}(GF, D_p). \quad (11)$$

Apparently, the relative contribution of less hygroscopic particles is the strongest in the interstitial population and the more hygroscopic mode appears distinctly only in the total and estimated residual aerosol. This is also reflected by the average growth factors. At D_p = 120~~ nm~~ and 150 nm, the GFs of cloud droplet residuals are approximately ~~10~~ 18% higher than those of interstitial particles. In terms of κ values, this discrepancy ~~corresponds~~would correspond to a difference up to ~~60–80~~ 65%–

75% depending on particle size. Again, it should be remarked that similar to activated fractions, the residual GF distributions (c_{res}) can appear locally negative if the interstitial concentrations are higher than the respective total concentrations. Before converting these distributions into GF-PDFs shown in Fig. 1, the negative values were set to zeros which eventually strengthened the positive peaks appearing in normalized distributions. As a result, for example the less hygroscopic particle mode appearing in the estimated residual aerosol can be partially attributed to methodological uncertainties.

To our knowledge, this is one of the very few studies characterizing the hygroscopic properties of different in-cloud aerosol populations. Previously, Svenningsson et al. (1994) studied the aerosol hygroscopicity and its relationship to cloud droplet activation at Kleiner Feldberg in Germany. Interstitial aerosol hygroscopicity was measured during cloud events, and by assuming that the air mass was the same, it was compared to the total aerosol sampled during the following clear sky conditions. The less hygroscopic particle fraction was substantially higher in the interstitial population, indicating that the more hygroscopic particles were scavenged into the cloud droplets more efficiently than the less hygroscopic ones. This observation was confirmed in a case study, where a counter flow virtual impactor (CVI) was used to separate the cloud droplets from ~~the~~ total aerosol, so that the hygroscopicity of cloud droplet residuals could be measured independently. Likewise, Rose et al. (2013) observed a decreasing fraction of available CCN during a precipitative cloud event, suggesting that the more hygroscopic particles were mostly activated into cloud droplets and removed from the air through precipitation. Overall, ~~the~~our results ~~by Svenningsson et al. (1994)~~from Puijo are in ~~a~~ good agreement with ~~our~~the observations ~~from Puijo.~~reported by Svenningsson et al. (1994) and Rose et al. (2013).

In situ aerosol chemical composition and partitioning between activated and non-activated particles has been studied recently by means of aerosol mass spectrometry (e.g. Hao et al., 2013; Zelenyuk at al., 2010; Kamphus et al., 2010; Drewnick et al., 2006) and electron microscopy (Li et al., 2011). Based on the results from Puijo Cloud Experiment 2010, Hao et al. (2013) reported substantially higher mass fractions of organic nitrate and less oxidized organic species in the interstitial particles compared to residual ones. Similarly, Zelenyuk et al. (2010) and Li et al. (2011) observed an elevated fraction of sulfates in the activated particles. Although these results are broadly in line with our observations on the ~~hygroscopic discrepancies observed in this study~~distinct hygroscopicity of activated and non-activated particles, great care should be taken when comparing the results. For example, Hao et al. (2013) observed an increased organic fraction in the Aitken mode particles, indicating that the differences in chemical composition also reflected the effect of particle size.

At Puijo, the critical droplet activation diameter, i.e. the diameter corresponding to the 50% activation efficiency (D50), varies typically between 100 and 200 nm. According to ~~the above results~~our observations, this value is highly dependent on the prevailing hygroscopicity. To illustrate this relationship, the DMPS derived D50s (obtained from $f_{act,DMPS}$ via linear interpolation) were correlated with ~~the~~ hourly averaged κ values. Furthermore, a non-linear regression model $D50 \sim a \times \kappa^{-1/3}$ was chosen to account for the theoretical dependence addressed in Eq. (5). ~~The results are summarized in Fig. 2, where the data points are colored according to the number fraction of less hygroscopic particles.~~Figure 3 summarizes the results from all the observed cloud hours. Since the average hygroscopicity reflects the relative contribution of the two GF modes, the low-end κ values were characterized by elevated $f_{GF<1.25}$ and vice versa. Differing more than three standard deviations from the

campaign average of 132 nm, the data point with D50 = 231 nm was excluded from the analysis as an outlier. Apart from this exception, the hourly D50s ranged from 93 to 173 nm.

The 80 nm particles yielded the weakest correlation with root-mean-square error (RMSE) of ~29 nm. This could be expected since the 80 nm size usually remained well below the critical activation limit. On the contrary, the 120 and 150 nm sizes yielded the RMSE values ~~of~~around ~13 nm, suggesting a considerably stronger correlation between the two parameters. According to the linear correlations reported by Quinn et al. (2008), the chemical composition (parametrized ~~by~~as HOA mass fraction) explained approximately 40% to 50~~-~~% of the variation in critical activation diameter. In ~~our case~~comparison, applying a linear regression to our data set would ~~lead to~~result in R^2 values of 0.58 (120 nm) and 0.57 (150 nm~~), indicating~~). Assuming that the ~~hygroscopicity of~~relationship between κ and D50 could be treated as (locally) linear, these values would indicate that the accumulation mode ~~particles~~ hygroscopicity explained up to 57~~–~~% ~~–~~58~~-~~% of the observed variance in D50, therefore dominating the effect of varying meteorology and especially, the varying supersaturation. Moreover, no correlation was found between the κ values and the estimated effective peak supersaturations ($R^2 \sim 0.02$; not shown here).

3.4 $N_{act,HTDMA}$ and ~~s_{eff}~~$s_{c,eff}$

The activation efficiency curves and the corresponding cloud droplet number concentrations were derived from the hourly averaged GF-PDFs according to the procedure described in Sect. 2.5. Reproducibility of the DMPS derived activation curves and cloud droplet nuclei spectra was confirmed visually, and the data points with considerable ~~uncertainties~~ differences were omitted from the ~~analysis. A~~following analyses. In most of these cases, the estimated activation curves appeared clearly steeper than the measured ones, leading to both an underestimation of activated fraction at D_p < D50 and an overestimation of activated fraction at D_p > D50. Alternatively, some of the estimated curves managed to reproduce the correct behavior at smaller sizes (D_p < 150 nm) but overestimated the activation at the size range of extrapolated GF-PDFs. Although these uncertainties caused only a small net bias to droplet estimations, they indicate that the estimated GF surfaces may have failed to replicate the real ambient conditions.

Figure 4 shows a comparison between the HTDMA and DMPS derived cloud droplet concentrations ~~is shown in Fig. 3~~ (red dots). The regression line fitted through the 26 data points has a slope of 1.~~03~~016 indicating a good agreement between the estimated and measured cloud droplet concentrations. In addition, Fig. ~~3~~4 includes a comparison between the external and the internal mixing approaches (grey dots). Correspondingly, the regression line has a slope of 1.022 and all the hourly data points lie between the ratios 0.91 and 1.04. ~~Similarly~~Analogous to Kammermann et al. (2010b), this observation suggests that the CCN concentration can be determined with reasonable accuracy even if the exact mixing state remains unknown. Nevertheless, since the determination of $N_{act,HTDMA}$ included the estimation of effective peak supersaturation by means of $f_{act,DMPS}$, the comparison shown here can't be considered as a real CCN closure study in an explicit manner. Instead, it rather serves as a base for the analysis presented in the following section (Sect. 3.5).

~~In this study~~Overall, the hourly estimated peak supersaturations ranged from 0.16% to 0.29~~ %.~~%. Apart of one exception with $s_{c,eff}$ up to 0.44%, this range was valid also for the omitted cloud hours. Although these values might be slightly biased due to

the ~~hygroscopicity related~~possible discrepancies between sub- and supersaturated hygroscopicities, they provide ~~some~~ valuable information about the ~~in-cloud~~ conditions~~.~~ relevant to cloud droplet formation. Reaching the average and median values of 0.22 ~~%, these~~%, the estimated $s_{c,eff}$ values are comparable to ~~the~~ supersaturations of 0.18 ~~%~~ 0.26 ~~%~~ obtained by Anttila et al. (2009) at the Pallas GAW station in Northern Finland. Similar "average" supersaturations can ~~also~~ be obtained also by using the regression curves presented in Fig. ~~2~~3. By assuming a constant temperature of 2 ~~.2~~ °C (average temperature of all the cloud ~~events~~hours), the regression parameters 6.94×10^{-8} (120 nm) and 7.52×10^{-8} (150 nm) imply supersaturations of 0.23 ~~.~~% and 0.20 ~~.~~%, respectively. ~~On the other hand~~By contrast, these values are somewhat low compared to the high-end supersaturations determined at some European ~~high altitude~~mountain sites. For example, ~~Hammer et al. (2014) reported a median peak supersaturation of 0.35 % for a mountain site at Jungfraujoch and similarly,~~ Asmi et al. (2012) found supersaturations ranging from 0.1% up to 0.6 ~~.~~% at Puy-de-Dôme~~.~~, and similarly, Hammer et al. (2014) observed a median peak supersaturation of 0.35% at Jungfraujoch. On the other hand, Hammer et al. (2014) also found a clear difference between the two dominant wind sectors reflecting the effect of terrain topography on updraft velocities. Generally, the air masses rising over the less steep mountainside were characterized by weaker updrafts and consequently, by supersaturations more comparable to ours (median 0.22%).

3.5 Sensitivity of cloud droplet formation to varying hygroscopicity

Following the procedure described in Sect. 2.5, we performed κ-Köhler simulations to investigate~~,~~ how the cloud droplet concentrations would change if all the particles belonged to the more hygroscopic group. For each cloud hour, we created an alternative hygroscopicity scenario by modifying the original GF-PDFs. This alteration was ~~done~~conducted by eliminating the contribution of ~~the~~ less hygroscopic particles and normalizing the resulting distributions so that the integral over each particle size became equal to one. In principle, the most significant changes appeared at sizes where the original $f_{GF<1.25}$ ~~was~~were large enough to be affected by the modifications. Thus, instead of varying the ~~growth factors~~GFs equally and regardless of particle size, the modifications only ~~effected~~affected the presence of an existing low-GF mode and increased the average GFs accordingly.

Overview of the applied hygroscopic variations is presented in Table 2. Shown are average GFs at D_p = 80, 120, 150 and 200 nm for the two hygroscopicity scenarios, as well as their absolute deviation from each other. In terms of κ values, the high hygroscopicity assumption results in values ~~lying~~ between 0.20 and 0.40. According to Andreae and Rosenfeld (2008), these values would be characteristic ~~for~~of typical aged continental aerosol. In order to highlight their atmospheric relevance, it's also important to note that they are within the range of hygroscopicities observed at Puijo during the campaign period. ~~In Fig. 4,~~The cloud droplet concentrations were calculated for both scenarios by using identical particle size distributions as well as equal effective peak supersaturations.

Figure 5 shows the relative and absolute changes in $N_{act,HTDMA}$ ~~are plotted~~ against the hygroscopicity shift at D_p = 150 nm. Again, the data points are colored according to the less hygroscopic fraction, and the marker size is scaled relative to total particle number concentration.

Naturally, the relative change in cloud droplet concentration increases with ~~an~~ increasing hygroscopicity~~ shift. The total variation extends up to 70 %, with~~. Although most of the data points ~~residing~~reside in the range of 10–%–40~~ %. Because~~%, the total variation extends up to 70%. Furthermore, because of the approximately linear behavior of relative $\Delta N_{act,HTDMA}$, the absolute change appears highly sensitive to initial particle size distribution. In the case of high total concentration, the absolute $\Delta N_{act,HTDMA}$ can be up to hundreds of droplets per cubic centimeter even with reasonably small hygroscopic variations ($\Delta GF_{150\ nm} < 0.10$). ~~In addition to droplet concentration, Fig. 4 illustrates the change in critical activation diameter (D50). Understandably, by suppressing the size-dependent variations in chemical composition, the activation curves become steeper and the D50s decrease. Typically, the change in D50 remains below 20 nm, but in the most extreme cases, it can be up to almost 35 nm.~~

In addition to droplet concentration, Fig. 5 illustrates the change in critical activation diameter ($D50_{HTDMA}$; derived from $f_{act,HTDMA}$ via linear interpolation). Understandably, as the high hygroscopicity assumption suppresses the size-dependence of aerosol hygroscopicity (see Table 2), the activation efficiency curves become steeper and D50s decrease. Typically, the change in D50 remains below 20 nm but can reach 35 nm in the most extreme cases.

Anttila et al. (2009) studied the effect of varying hygroscopicity at the Pallas GAW station in Northern Finland. According to the simulations, increasing the GFs by 10-% led to 17–%–51-% increments in cloud droplet number concentration. Bearing in mind that ~~the~~a 10-% relative change in GFs corresponded to an absolute change of ~0.13 at D_p = 150 nm, the observations by Anttila et al. (2009) are in ~~a~~ good agreement with ~~the~~our results~~ reported above.~~. However, it is also worth pointing out~~,~~ that by increasing all the GFs by 10-%, the absolute change in ~~hygroscopicity~~growth factors increased with particle size. In our analysis, removal of the less hygroscopic mode induced the opposite effect.

~~Similarly~~Similar to our analysis, Wex et al. (2010) assessed the overestimation of CCN concentration if all the particles were assumed to have κ of the more hygroscopic particles. By using data from the literature~~ data~~, the overestimation was derived for rural, urban and marine aerosol populations and for different less hygroscopic fractions. In the case of urban and rural aerosols, the overestimation varied between 20–%–40-% and 40–%–100-% when the less hygroscopic fraction ($\kappa < 0.10$) was set to 0.3 and 0.5, respectively. With the range of variation illustrating the inverse proportionality to supersaturation (~~s~~ =between 0.1–% and 0.5-%), these values are comparable to our observations. However, Wex et al. (2010) assumed the same less hygroscopic fraction for all particle sizes, which is very rarely the case in our conditions at Puijo.

~~In addition,~~ Kammermann et al. (2010b) performed a set of CCN closure studies to investigate the sensitivity of CCN concentration to unknown chemical composition. ~~According to the results, the~~The median bias between the predicted and measured CCN concentrations was up to +54–% when a constant κ = 0.30 was assumed. ~~Similarly~~Analogous to our ~~measurement site~~observations, the average hygroscopicities reported by Kammermann et al. (2010b) were relatively low explaining the remarkable bias in CCN predictions. On the contrary, Meng et al. (2014) found a reasonably good agreement between the measured and predicted CCN concentrations by using a constant κ as high as 0.33 at a coastal site in Hong Kong, where the aerosol composition was dominated by inorganic species.

In principle, the high hygroscopicity assumption yields ~~in~~ values resembling the hygroscopicities that could be obtained from bulk composition measurements by means of aerosol mass spectrometry. Typically, the bulk composition is biased towards the inorganics ~~because of~~due to the emphasis on larger particles. This can lead to a considerable overestimation of CCN concentration. For example, Medina et al. (2007), Almeida et al. (2013) and Meng et al. (2014) reported an overprediction of 26 %–44 % at ~0.20 % supersaturation when only the size-averaged composition was ~~taken into account.~~considered. In all of these studies, implementing the size-dependent or size-resolved chemical composition substantially improved the CCN predictions ~~substantially~~.

4 Summary and conclusions

The relationship between aerosol hygroscopicity and cloud droplet activation was studied at the Puijo measurement station in Kuopio, Finland during the Puijo Cloud Experiment 2014. The purpose of the campaign was to identify the hygroscopicity-dependent activation properties of cloud forming aerosol population, as well as to study the sensitivity of cloud droplet activation to varying chemical composition in real atmospheric in-cloud conditions. In total, 15 cloud events were observed during the 2-month long campaign providing a total of 47 cloud hours.

The aerosol hygroscopicity at 90 % RH was measured with an HTDMA. Typically, the measured GF-PDFs appeared bimodal, indicating an externally mixed aerosol population. By using the GF-PDFs and particle concentrations measured separately for interstitial and total aerosol populations, the hygroscopicity-dependent activation properties were estimated. The growth factor distributions were divided into low and high hygroscopicity regimes by using ~~the~~a GF limit of 1.25 and the activated fraction in each category was ~~calculated~~estimated.

The in-cloud measurements revealed clear differences in activation efficiency between the two GF modes. The less hygroscopic particles originating most likely from local anthropogenic sources remained ~~almost~~mostly non-activated, ~~while~~whereas the more hygroscopic mode was primarily scavenged into cloud droplets. This observation highlights the role of aerosol hygroscopicity and chemical composition in cloud droplet activation. A highly variable portion of less hygroscopic particles have been reported in several studies and in many different locations during the last few decades. Due to the anthropogenic contribution, the less hygroscopic mode can be dominant at particle sizes up to 250 nm. As shown by our analysis, this can lead to a significant decrease in the fraction of available CCN.

By modifying the measured GF-PDFs, we estimated~~,~~ how the cloud droplet ~~concentration~~concentrations would change if all the particles belonged to the more hygroscopic mode. This would correspond to a situation with typical aged, continental aerosol in the atmosphere without any fresh anthropogenic influence. According to the κ-Köhler simulations, the change in cloud droplet concentration was up to 70 ~~% depending~~% when the possible feedback effects on ~~the increase in hygroscopicity.~~cloud supersaturation were assumed negligible. Our result clearly demonstrates the importance of correct treatment of anthropogenic organic aerosols, their hygroscopicity and the effect of atmospheric aging, when estimating ~~the~~ CCN ~~concentration~~concentrations.

Acknowledgements. This work was supported by the European Research Council (ERC starting grant 335478), the Academy of Finland (grant no. 272041, 259005, 283031) and The Doctoral School of the University of Eastern Finland. In addition, A.R. acknowledges the financial support from Maj and Tor Nessling Foundation.

References

Ahmad, I., Mielonen, T., Grosvenor, D. P., Portin, H. J., Arola, A., Mikkonen, S., Kuhn, T., Leskinen, A., Joutsensaari, J., Komppula, M., Lehtinen, K. E. J., Laaksonen, A., and Romakkaniemi, S.: Long-term measurements of cloud droplet concentrations and aerosol-cloud interactions in continental boundary layer clouds, Tellus B, 65, 20138, doi:10.3402/Tellusb.V65i0.20138, 2013.

Almeida, G. P., Brito, J., Morales, C. A., Andrade, M. F., and Artaxo, P.: Measured and modelled cloud condensation nuclei (CCN) concentration in Sao Paulo, Brazil: the importance of aerosol size-resolved chemical composition on CCN concentration prediction, Atmos. Chem. Phys., 14, 7559-7572, doi:10.5194/acp-14-7559-2014, 2014.

Andreae, M. O., and Rosenfeld, D.: Aerosol-cloud-precipitation interactions. Part 1. The nature and sources of cloud-active aerosols, Earth.-Sci. Rev., 89, 13-41, doi:10.1016/j.earscirev.2008.03.001, 2008.

Anttila, T., Vaattovaara, P., Komppula, M., Hyvarinen, A. P., Lihavainen, H., Kerminen, V. M., and Laaksonen, A.: Size-dependent activation of aerosols into cloud droplets at a subarctic background site during the second Pallas Cloud Experiment (2nd PaCE): method development and data evaluation, Atmos. Chem. Phys., 9, 4841-4854, 2009.

Asmi, E., Freney, E., Hervo, M., Picard, D., Rose, C., Colomb, A., and Sellegri, K.: Aerosol cloud activation in summer and winter at puy-de-Dome high altitude site in France, Atmos. Chem. Phys., 12, 11589-11607, doi:10.5194/acp-12-11589-2012, 2012.

Broekhuizen, K., Chang, R. Y. W., Leaitch, W. R., Li, S. M., and Abbatt, J. P. D.: Closure between measured and modeled cloud condensation nuclei (CCN) using size-resolved aerosol compositions in downtown Toronto, Atmos. Chem. Phys., 6, 2513-2524, 2006.

Conant, W. C., VanReken, T. M., Rissman, T. A., Varutbangkul, V., Jonsson, H. H., Nenes, A., Jimenez, J. L., Delia, A. E., Bahreini, R., Roberts, G. C., Flagan, R. C., and Seinfeld, J. H.: Aerosol-cloud drop concentration closure in warm cumulus, J. Geophys. Res.-Atmos., 109, D13204, doi:10.1029/2003jd004324, 2004.

Drewnick, F., Schneider, J., Hings, S. S., Hock, N., Noone, K., Targino, A., Weimer, S., and Borrmann, S.: Measurement of ambient, interstitial, and residual aerosol particles on a mountaintop site in central Sweden using an aerosol mass spectrometer and a CVI, J. Atmos. Chem., 56, 1-20, doi:10.1007/s10874-006-9036-8, 2007.

Dusek, U., Frank, G. P., Hildebrandt, L., Curtius, J., Schneider, J., Walter, S., Chand, D., Drewnick, F., Hings, S., Jung, D., Borrmann, S., and Andreae, M. O.: Size matters more than chemistry for cloud-nucleating ability of aerosol particles, Science, 312, 1375-1378, doi:10.1126/science.1125261, 2006.

Ervens, B., Cubison, M., Andrews, E., Feingold, G., Ogren, J. A., Jimenez, J. L., DeCarlo, P., and Nenes, A.: Prediction of cloud condensation nucleus number concentration using measurements of aerosol size distributions and composition and light scattering enhancement due to humidity, J. Geophys. Res.-Atmos., 112, D10s32, doi:10.1029/2006jd007426, 2007.

Ferron, G. A., Karg, E., Busch, B., and Heyder, J.: Ambient particles at an urban, semi-urban and rural site in Central Europe: hygroscopic properties, Atmos. Environ., 39, 343-352, doi:10.1016/j.atmosenv.2004.09.015, 2005.

Fitzgerald, J.: Dependence of the Supersaturation Spectrum of CCN on Aerosol Size Distribution and Composition, J. Atmos. Sci., 30, 628-634, doi:http://dx.doi.org/10.1175/1520-0469(1973)030<0628:DOTSSO>2.0.CO;2, 1973.

Fors, E. O., Swietlicki, E., Svenningsson, B., Kristensson, A., Frank, G. P., and Sporre, M.: Hygroscopic properties of the ambient aerosol in southern Sweden - a two year study, Atmos. Chem. Phys., 11, 8343-8361, doi:10.5194/acp-11-8343-2011, 2011.

Fountoukis, C., Nenes, A., Meskhidze, N., Bahreini, R., Conant, W. C., Jonsson, H., Murphy, S., Sorooshian, A., Varutbangkul, V., Brechtel, F., Flagan, R. C., and Seinfeld, J. H.: Aerosol-cloud drop concentration closure for clouds sampled during the International Consortium for Atmospheric Research on Transport and Transformation 2004 campaign, J. Geophys. Res.-Atmos., 112, D10s30, doi:10.1029/2006jd007272, 2007.

Good, N., Topping, D. O., Allan, J. D., Flynn, M., Fuentes, E., Irwin, M., Williams, P. I., Coe, H., and McFiggans, G.: Consistency between parameterisations of aerosol hygroscopicity and CCN activity during the RHaMBLe discovery cruise, Atmos. Chem. Phys., 10, 3189-3203, 2010.

Gysel, M., McFiggans, G. B., and Coe, H.: Inversion of tandem differential mobility analyser (TDMA) measurements, J Aerosol Sci., 40, 134-151, doi:10.1016/j.jaerosci.2008.07.013, 2009.

Hammer, E., Bukowiecki, N., Gysel, M., Juranyi, Z., Hoyle, C. R., Vogt, R., Baltensperger, U., and Weingartner, E.: Investigation of the effective peak supersaturation for liquid-phase clouds at the high-alpine site Jungfraujoch, Switzerland (3580 m a.s.l.), Atmos. Chem. Phys., 14, 1123-1139, doi:10.5194/acp-14-1123-2014, 2014.

Hao, L. Q., Romakkaniemi, S., Kortelainen, A., Jaatinen, A., Portin, H., Miettinen, P., Komppula, M., Leskinen, A., Virtanen, A., Smith, J. N., Sueper, D., Worsnop, D. R., Lehtinen, K. E. J., and Laaksonen, A.: Aerosol Chemical Composition in Cloud Events by High Resolution Time-of-Flight Aerosol Mass Spectrometry, Environ. Sci. Technol., 47, 2645-2653, doi:10.1021/es302889w, 2013.

Henning, S., Dieckmann, K., Ignatius, K., Schafer, M., Zedler, P., Harris, E., Sinha, B., van Pinxteren, D., Mertes, S., Birmili, W., Merkel, M., Wu, Z., Wiedensohler, A., Wex, H., Herrmann, H., and Stratmann, F.: Influence of cloud processing on CCN activation behaviour in the Thuringian Forest, Germany during HCCT-2010, Atmos. Chem. Phys., 14, 7859-7868, doi:10.5194/acp-14-7859-2014, 2014.

Hersey, S. P., Craven, J. S., Metcalf, A. R., Lin, J., Lathem, T., Suski, K. J., Cahill, J. F., Duong, H. T., Sorooshian, A., Jonsson, H. H., Shiraiwa, M., Zuend, A., Nenes, A., Prather, K. A., Flagan, R. C., and Seinfeld, J. H.: Composition and hygroscopicity of the Los Angeles Aerosol: CalNex, J. Geophys. Res.-Atmos., 118, 3016-3036, doi:10.1002/jgrd.50307, 2013.

Hudson, J. G.: Variability of the relationship between particle size and cloud-nucleating ability, Geophys. Res. Lett., 34, L08801, doi:10.1029/2006gl028850, 2007.

IPCC: Climate change 2013: The physical science basis. Intergovernmental panel on Climate Change, Cambridge University Press, New York, 2013.

Jaatinen, A., Romakkaniemi, S., Anttila, T., Hyvarinen, A. P., Hao, L. Q., Kortelainen, A., Miettinen, P., Mikkonen, S., Smith, J. N., Virtanen, A., and Laaksonen, A.: The third Pallas Cloud Experiment: Consistency between the aerosol hygroscopic growth and CCN activity, Boreal Environ. Res., 19, 368-382, 2014.

Junge, C. M., E.: Relationship of Cloud Nuclei Spectra to Aerosol Size Distribution and Composition, J. Atmos. Sci., 28, 282-390, 1971.

Juranyi, Z., Tritscher, T., Gysel, M., Laborde, M., Gomes, L., Roberts, G., Baltensperger, U., and Weingartner, E.: Hygroscopic mixing state of urban aerosol derived from size-resolved cloud condensation nuclei measurements during the MEGAPOLI campaign in Paris, Atmos. Chem. Phys., 13, 6431-6446, doi:10.5194/acp-13-6431-2013, 2013.

Kammermann, L., Gysel, M., Weingartner, E., and Baltensperger, U.: 13-month climatology of the aerosol hygroscopicity at the free tropospheric site Jungfraujoch (3580 m a.s.l.), Atmos. Chem. Phys., 10, 10717-10732, doi:10.5194/acp-10-10717-2010, 2010a.

Kammermann, L., Gysel, M., Weingartner, E., Herich, H., Cziczo, D. J., Holst, T., Svenningsson, B., Arneth, A., and Baltensperger, U.: Subarctic atmospheric aerosol composition: 3. Measured and modeled properties of cloud condensation nuclei, J. Geophys. Res.-Atmos., 115, D04202, doi:10.1029/2009jd012447, 2010b.

Kamphus, M., Ettner-Mahl, M., Klimach, T., Drewnick, F., Keller, L., Cziczo, D. J., Mertes, S., Borrmann, S., and Curtius, J.: Chemical composition of ambient aerosol, ice residues and cloud droplet residues in mixed-phase clouds: single particle analysis during the Cloud and Aerosol Characterization Experiment (CLACE 6), Atmos. Chem. Phys., 10, 8077-8095, doi:10.5194/acp-10-8077-2010, 2010.

Komppula, M., Lihavainen, H., Kerminen, V. M., Kulmala, M., and Viisanen, Y.: Measurements of cloud droplet activation of aerosol particles at a clean subarctic background site, J. Geophys. Res.-Atmos., 110, D06204, doi:10.1029/2004jd005200, 2005.

Köhler, H.: The nucleus in and the growth of hygroscopic droplets, Trans. Faraday Soc., 32, 1152-1161, doi:10.1039/TF9363201152, 1936.

Laborde, M., Crippa, M., Tritscher, T., Juranyi, Z., Decarlo, P. F., Temime-Roussel, B., Marchand, N., Eckhardt, S., Stohl, A., Baltensperger, U., Prevot, A. S. H., Weingartner, E., and Gysel, M.: Black carbon physical properties and mixing state in the European megacity Paris, Atmos. Chem. Phys., 13, 5831-5856, doi:10.5194/acp-13-5831-2013, 2013.

Leskinen, A., Portin, H., Komppula, M., Miettinen, P., Arola, A., Lihavainen, H., Hatakka, J., Laaksonen, A., and Lehtinen, K. E. J.: Overview of the research activities and results at Puijo semi-urban measurement station, Boreal Environ. Res., 14, 576-590, 2009.

Leskinen, A., Arola, A., Komppula, M., Portin, H., Tiitta, P., Miettinen, P., Romakkaniemi, S., Laaksonen, A., and Lehtinen, K. E. J.: Seasonal cycle and source analyses of aerosol optical properties in a semi-urban environment at Puijo station in Eastern Finland, Atmos. Chem. Phys., 12, 5647-5659, doi:10.5194/acp-12-5647-2012, 2012.

Li, W. J., Li, P. R., Sun, G. D., Zhou, S. Z., Yuan, Q., and Wang, W. X.: Cloud residues and interstitial aerosols from non-precipitating clouds over an industrial and urban area in northern China, Atmos. Environ., 45, 2488-2495, doi:10.1016/j.atmosenv.2011.02.044, 2011.

Liu, P. F., Zhao, C. S., Gobel, T., Hallbauer, E., Nowak, A., Ran, L., Xu, W. Y., Deng, Z. Z., Ma, N., Mildenberger, K., Henning, S., Stratmann, F., and Wiedensohler, A.: Hygroscopic properties of aerosol particles at high relative humidity and their diurnal variations in the North China Plain, Atmos. Chem. Phys., 11, 3479-3494, doi:10.5194/acp-11-3479-2011, 2011.

Liu, D., Allan, J., Whitehead, J., Young, D., Flynn, M., Coe, H., McFiggans, G., Fleming, Z. L., and Bandy, B.: Ambient black carbon particle hygroscopic properties controlled by mixing state and composition, Atmos. Chem. Phys., 13, 2015-2029, doi:10.5194/acp-13-2015-2013, 2013.

McFiggans, G., Artaxo, P., Baltensperger, U., Coe, H., Facchini, M. C., Feingold, G., Fuzzi, S., Gysel, M., Laaksonen, A., Lohmann, U., Mentel, T. F., Murphy, D. M., O'Dowd, C. D., Snider, J. R., and Weingartner, E.: The effect of physical and chemical aerosol properties on warm cloud droplet activation, Atmos. Chem. Phys., 6, 2593-2649, 2006.

Medina, J., Nenes, A., Sotiropoulou, R. E. P., Cottrell, L. D., Ziemba, L. D., Beckman, P. J., and Griffin, R. J.: Cloud condensation nuclei closure during the International Consortium for Atmospheric Research on Transport and Transformation 2004 campaign: Effects of size-resolved composition, J. Geophys. Res.-Atmos., 112, D10s31, doi:10.1029/2006jd007588, 2007.

Meng, J. W., Yeung, M. C., Li, Y. J., Lee, B. Y. L., and Chan, C. K.: Size-resolved cloud condensation nuclei (CCN) activity and closure analysis at the HKUST Supersite in Hong Kong, Atmos. Chem. Phys., 14, 10267-10282, doi:10.5194/acp-14-10267-2014, 2014.

Pajunoja, A., Lambe, A. T., Hakala, J., Rastak, N., Cummings, M. J., Brogan, J. F., Hao, L. Q., Paramonov, M., Hong, J., Prisle, N. L., Malila, J., Romakkaniemi, S., Lehtinen, K. E. J., Laaksonen, A., Kulmala, M., Massoli, P., Onasch, T. B., Donahue, N. M., Riipinen, I., Davidovits, P., Worsnop, D. R., Petaja, T., and Virtanen, A.: Adsorptive uptake of water by semisolid secondary organic aerosols, Geophys. Res. Lett., 42, 3063-3068, doi:10.1002/2015GL063142, 2015.

Petters, M. D., and Kreidenweis, S. M.: A single parameter representation of hygroscopic growth and cloud condensation nucleus activity, Atmos. Chem. Phys., 7, 1961-1971, 2007.

Portin, H. J., Komppula, M., Leskinen, A. P., Romakkaniemi, S., Laaksonen, A., and Lehtinen, K. E. J.: Observations of aerosol-cloud interactions at the Puijo semi-urban measurement station, Boreal Environ. Res., 14, 641-653, 2009.

Portin, H., Leskinen, A., Hao, L., Kortelainen, A., Miettinen, P., Jaatinen, A., Laaksonen, A., Lehtinen, K. E. J., Romakkaniemi, S., and Komppula, M.: The effect of local sources on particle size and chemical composition and their role in aerosol-cloud interactions at Puijo measurement station, Atmos. Chem. Phys., 14, 6021-6034, doi:10.5194/acp-14-6021-2014, 2014.

Quinn, P. K., Bates, T. S., Coffman, D. J., and Covert, D. S.: Influence of particle size and chemistry on the cloud nucleating properties of aerosols, Atmos. Chem. Phys., 8, 1029-1042, doi:10.5194/acp-8-1029-2008, 2008.

Rose, D., Gunthe, S. S., Jurányi, Z., Gysel, M., Frank, G. P., Schneider, J., Curtius, J., and Pöschl, U.: Size-resolved and integral measurements of cloud condensation nuclei (CCN) at the high-alpine site Jungfraujoch, Atmos. Chem. Phys. Discuss., 13, 32575-32624, doi:10.5194/acpd-13-32575-2013, 2013.

Sjogren, S., Gysel, M., Weingartner, E., Alfarra, M. R., Duplissy, J., Cozic, J., Crosier, J., Coe, H., and Baltensperger, U.: Hygroscopicity of the submicrometer aerosol at the high-alpine site Jungfraujoch, 3580 m a.s.l., Switzerland, Atmos. Chem. Phys., 8, 5715-5729, 2008.

Svenningsson, B., Hansson, H. C., Wiedensohler, A., Noone, K., Ogren, J., Hallberg, A., and Colvile, R.: Hygroscopic Growth of Aerosol-Particles and Its Influence on Nucleation Scavenging in-Cloud - Experimental Results from Kleiner-Feldberg, J. Atmos. Chem., 19, 129-152, doi:10.1007/Bf00696586, 1994.

Tiitta, P., Miettinen, P., Vaattovaara, P., Joutsensaari, J., Petaja, T., Virtanen, A., Raatikainen, T., Aalto, P., Portin, H., Romakkaniemi, S., Kokkola, H., Lehtinen, K. E. J., Kulmala, M., and Laaksonen, A.: Roadside aerosol study using hygroscopic, organic and volatility TDMAs: Characterization and mixing state, Atmos. Environ., 44, 976-986, doi:10.1016/j.atmosenv.2009.06.021, 2010.

Weingartner, E., Burtscher, H., and Baltensperger, U.: Hygroscopic properties of carbon and diesel soot particles, Atmos. Environ., 31, 2311-2327, doi:10.1016/S1352-2310(97)00023-X, 1997.

Wex, H., McFiggans, G., Henning, S., and Stratmann, F.: Influence of the external mixing state of atmospheric aerosol on derived CCN number concentrations, Geophys. Res. Lett., 37, L10805, doi:10.1029/2010gl043337, 2010.

Wiedensohler, A., Birmili, W., Nowak, A., Sonntag, A., Weinhold, K., Merkel, M., Wehner, B., Tuch, T., Pfeifer, S., Fiebig, M., Fjaraa, A. M., Asmi, E., Sellegri, K., Depuy, R., Venzac, H., Villani, P., Laj, P., Aalto, P., Ogren, J. A., Swietlicki, E., Williams, P., Roldin, P., Quincey, P., Huglin, C., Fierz-Schmidhauser, R., Gysel, M., Weingartner, E., Riccobono, F., Santos, S., Gruning, C., Faloon, K., Beddows, D., Harrison, R. M., Monahan, C., Jennings, S. G., O'Dowd, C. D., Marinoni, A., Horn, H. G., Keck, L., Jiang, J., Scheckman, J., McMurry, P. H., Deng, Z., Zhao, C. S., Moerman, M., Henzing, B., de Leeuw, G., Loschau, G., and Bastian, S.: Mobility particle size spectrometers: harmonization of technical standards and data structure to facilitate high quality long-term observations of atmospheric particle number size distributions, Atmos. Meas. Tech., 5, 657-685, doi:10.5194/amt-5-657-2012, 2012.

Winklmayr, W., Reischl, G. P., Lindner, A. O., and Berner, A.: A New Electromobility Spectrometer for the Measurement of Aerosol Size Distributions in the Size Range from 1 to 1000 Nm, J. Aerosol Sci., 22, 289-296, doi:10.1016/S0021-8502(05)80007-2, 1991.

Vlasenko, A., Sjogren, S., Weingartner, E., Gaggeler, H. W., and Ammann, M.: Generation of submicron Arizona test dust aerosol: Chemical and hygroscopic properties, Aerosol. Sci. Tech., 39, 452-460, doi:10.1080/02786290959870, 2005.

Zelenyuk, A., Imre, D., Earle, M., Easter, R., Korolev, A., Leaitch, R., Liu, P., Macdonald, A. M., Ovchinnikov, M., and Strapp, W.: In Situ Characterization of Cloud Condensation Nuclei, Interstitial, and Background Particles Using the Single Particle Mass Spectrometer, SPLAT II, Anal. Chem., 82, 7943-7951, doi:10.1021/ac1013892, 2010.

Table 1: Overview of the ~~three~~four cloud events observed during the measurement campaign. Given are the total particle and cloud droplet number concentrations as well as the hygroscopicity-~~segregated~~dependent activation efficiencies and growth factors of 120 and 150 nm particles. The number fraction of less hygroscopic particles is denoted by $f_{GF<1.25}$.

	Event #1		Event #2		Event #3		Event #4	
Time	08.10/20:46–23:45		11.10/20:25–21:56		13.10/05:57–07:40		20.10/00:01–04:26	
N_{tot}	2935 cm^{-3}		699 cm^{-3}		1442 cm^{-3}		792 cm^{-3}	
N_{act}	781 cm^{-3}		135 cm^{-3}		158 cm^{-3}		69 cm^{-3}	
	120 nm	150 nm	120 nm	150 nm	120 nm	150 nm	120 nm	150 nm
$f_{act,DMPS}$	0.20	0.40	0.29	0.55	0.37	0.68	0.39	0.68
$f_{act,GF\geq0.80}$	0.32	0.48	0.29	0.55	0.52	0.72	0.39	0.68
$f_{act,GF<1.25}$	0	0	0	0.31	0	0	0.04	0.34
$f_{act,GF\geq1.25}$	0.57	0.80	0.69	0.77	0.60	0.79	0.70	0.83
$GF_{avg,GF\geq0.80}$	1.27	1.31	1.20	1.25	1.58	1.65	1.27	1.41
$GF_{avg,GF<1.25}$	1.13	1.13	1.05	1.06	1.00	1.00	1.01	1.02
$GF_{avg,GF\geq1.25}$	1.38	1.42	1.41	1.42	1.68	1.71	1.50	1.58
$f_{GF<1.25}$	0.44	0.39	0.58	0.47	0.14	0.08	0.48	0.31

Table 2: The average GFs for reference and high hygroscopicity scenarios and their absolute deviation from each other. The values shown in the parentheses correspond to the minimum and maximum values. The GFs for D_p = 80, 120 and 150 nm originate from direct measurements, whereas the data for D_p = 200 nm is obtained via extrapolation.

	80 nm	120 nm	150 nm	200 nm
GF_{avg} [Reference]	1.20 (1.04/1.29)	1.30 (1.18/1.43)	1.38 (1.25/1.49)	1.44 (1.27/1.58)
GF_{avg} [High-GF]	1.40 (1.33/1.59)	1.43 (1.36/1.57)	1.47 (1.39/1.59)	1.49 (1.4/1.61)
ΔGF_{avg}	0.20 (0.07/0.43)	0.13 (0.06/0.24)	0.09 (0.04/0.21)	0.05 (0/0.15)

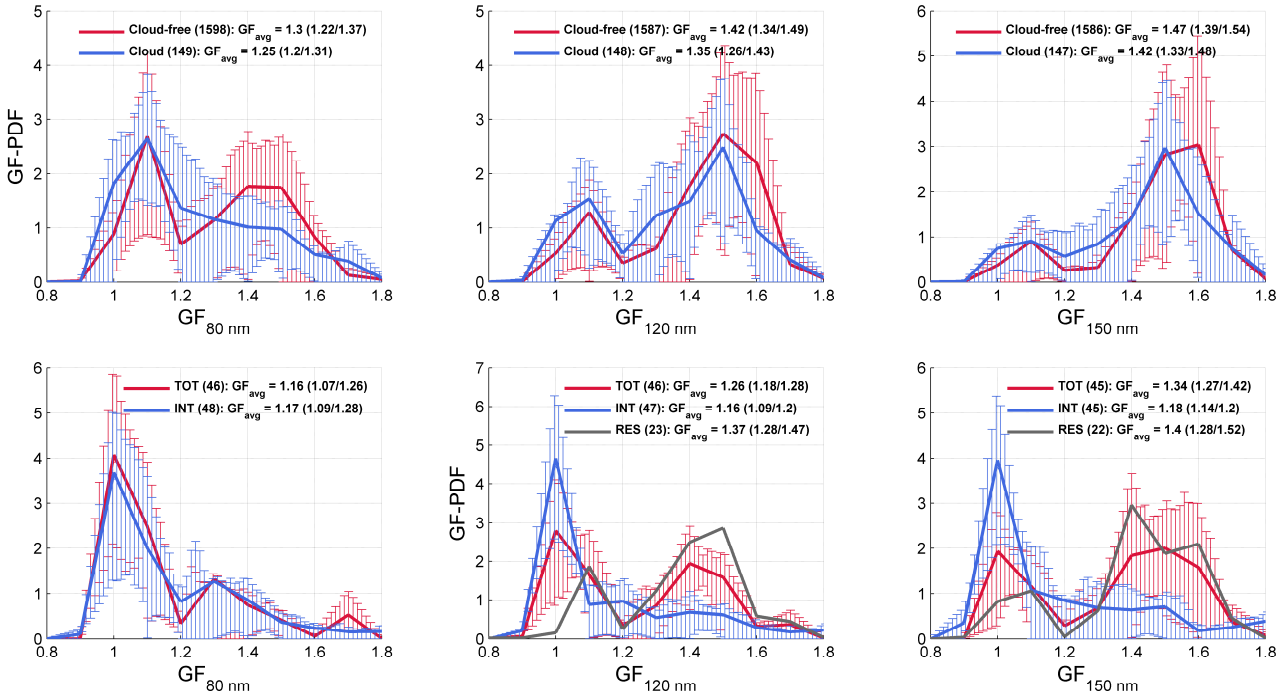

Figure 1: Top row: Average hygroscopicity of total aerosol at 90-% RH during cloudy (blue) and cloud-free (red) conditions (whole campaign). Bottom row: Average in-cloud hygroscopicity of total (red), interstitial (blue) and residual aerosol (black) during the ~~changing~~twin inlet period. The values shown in the parentheses represent the number of averaged observations and the 25th and 75th percentiles. In the graphs, the lower and upper quartiles are illustrated with whiskers.

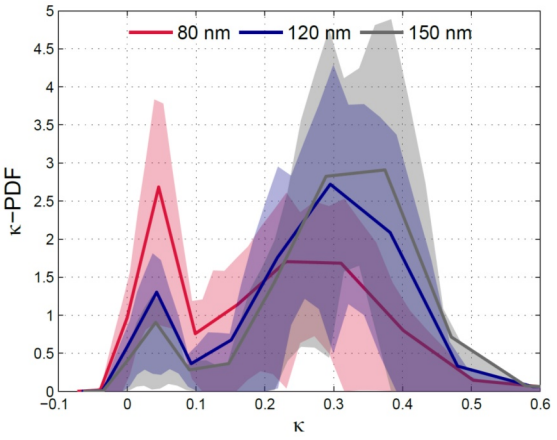

Figure 2: Mean κ-PDFs of 80, 120 and 150 nm particles calculated over the whole data set. The shaded areas represent the ranges between the 25th and 75th percentiles.

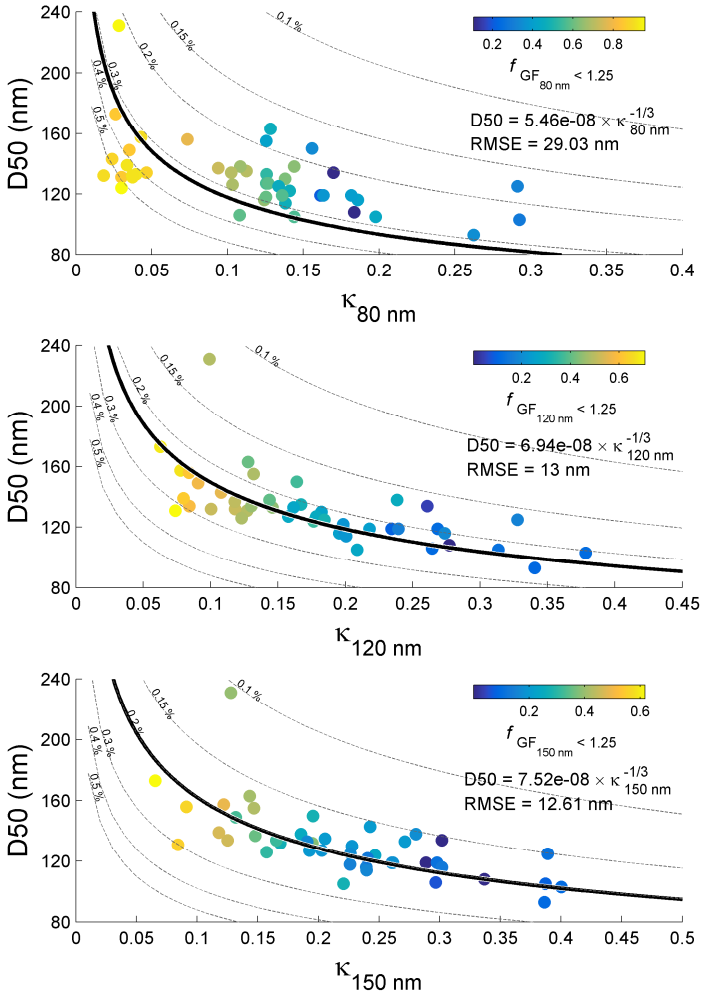

Figure 3: Critical activation diameter (D50) vs. size-averaged hygroscopicity (κ) of 80 nm, 120 nm and 150 nm particles, as well as the power law fits (black lines) to the data. The data points are colored according to number fraction of less hygroscopic particles, and the grey dashed lines represent the numerical solutions of Köhler theory in the range of s_c = 0.1%–0.5%.

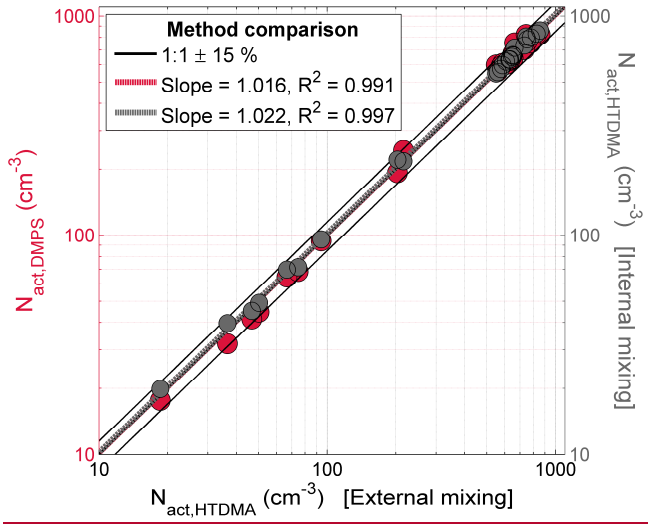

Figure ~~34~~. Correlations between the estimated (HTDMA) and measured (DMPS) cloud droplet concentrations (red dots) and the external and internal mixing approaches (grey dots). Each data point represents an hourly average.

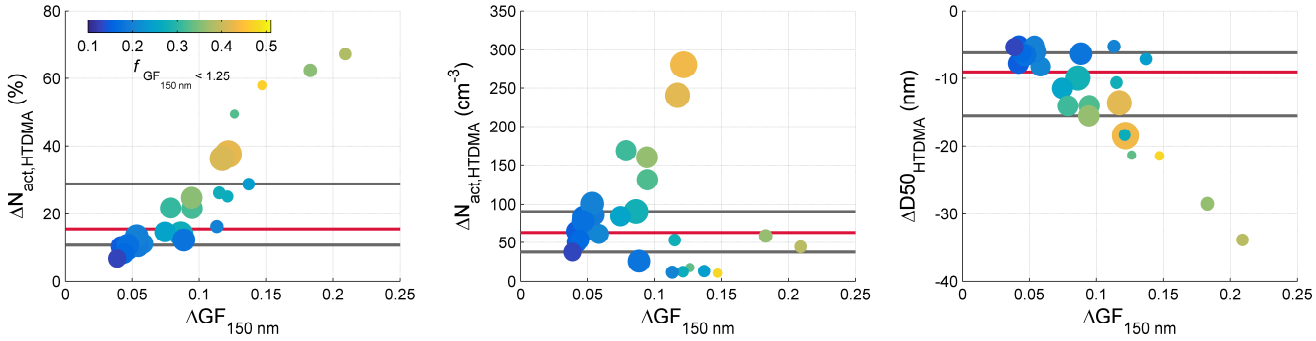

Figure 45: Simulated changes in cloud droplet number concentration ($N_{act,HTDMA}$) and critical activation diameter (~~D50~~$D50_{HTDMA}$) if all the particles belonged to the more hygroscopic mode. The marker size illustrates the total particle concentration in the range of 388 cm^{-3} to 3316 cm^{-3} and the data points are colored according to the less hygroscopic fraction (i.e. the fraction of particles merged into the more hygroscopic mode). The horizontal lines correspond to the 25th, 50th and 75th percentiles.